NAVAL POSTGRADUATE SCHOOL
MONTEREY, CALIFORNIA

THESIS

A PATCHED-CONIC ANALYSIS FOR OPTIMALLY DEFLECTING EARTH-CROSSING ASTEROIDS

by

Scott D. V. Porter

December 1997

Thesis Advisor: I. Michael Ross

1. AGENCY USE ONLY *(Leave blank)*	2. REPORT DATE December 1997	3. REPORT TYPE AND DATES COVERED Master's Thesis	
4. TITLE AND SUBTITLE A PATCHED-CONIC ANALYSIS FOR OPTIMALLY DEFLECTING EARTH-CROSSING ASTEROIDS			5. FUNDING NUMBERS
6. AUTHOR(S) Scott D. V. Porter			
7. PERFORMING ORGANIZATION NAME(S) AND ADDRESS(ES) Naval Postgraduate School Monterey CA 93943-5000			8. PERFORMING ORGANIZATION REPORT NUMBER
9. SPONSORING/MONITORING AGENCY NAME(S) AND ADDRESS(ES)			10. SPONSORING/MONITORING AGENCY REPORT NUMBER

11. SUPPLEMENTARY NOTES The views expressed in this thesis are those of the author and do not reflect the official policy or position of the Department of Defense or the U.S. Government.

12a. DISTRIBUTION/AVAILABILITY STATEMENT Approved for public release; distribution is unlimited.	12b. DISTRIBUTION CODE

13. ABSTRACT *(maximum 200 words)*

The threat of collision between an asteroid or a comet and the Earth has been well documented. Mitigation of such a threat can be accomplished by destruction of the threat or by perturbing the threat object into a safe orbit. Following a summary of proposed mitigation techniques, this thesis investigates the impulse required to safely perturb a threatening Earth-Crossing Asteroid (ECA). While previously published analysis included only two-body approximations to the impact geometry, this thesis adds the effect of the Earth's gravitational field to more closely approximate reality. The results indicate that third-body effects are strongest on ECA's in a nearly circular heliocentric orbit, where the minimum required ΔV can be several times larger than that calculated using two-body approximations. To determine the minimum ΔV required for mitigation, MATLAB®'s sequential quadratic programming (SQP) algorithm is applied to a constrained optimization problem. Third-body effects were added to a previously published two-body optimization by modifying the boundary conditions. With knowledge of the minimum ΔV requirements, the capability of current impulsive mitigation technology is analyzed. For asteroids of median density in co-planar orbits, a single 24 Mt nuclear explosive impulse applied earlier than 3 years before impact can effectively mitigate a threat with a diameter of 6 km. The capability significantly decreases with shorter warning times.

14. SUBJECT TERMS Earth-Crossing Asteroid, Near Earth Object, NEO Hazard Mitigation, Deflection, Asteroid, Comet, Impact Hazard, Optimum.	15. NUMBER OF PAGES 102
	16. PRICE CODE

17. SECURITY CLASSIFICATION OF REPORT Unclassified	18. SECURITY CLASSIFICATION OF THIS PAGE Unclassified	19. SECURITY CLASSIFICATION OF ABSTRACT Unclassified	20. LIMITATION OF ABSTRACT UL

A PATCHED-CONIC ANALYSIS FOR OPTIMALLY DEFLECTING EARTH-CROSSING ASTEROIDS

Scott D. V. Porter

Lieutenant, United States Navy

B.S., United States Naval Academy, 1989

Submitted in partial fulfillment

of the requirements for the degree of

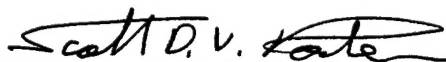## MASTER OF SCIENCE IN ASTRONAUTICAL ENGINEERING

from the

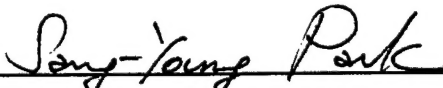## NAVAL POSTGRADUATE SCHOOL

December 1997

Author: _____
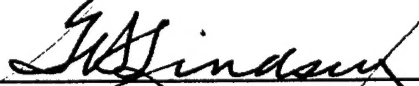
Scott D. V. Porter

Approved by: _____

I. M. Ross, Thesis Advisor

_____

S.-Y. Park, Second Reader

_____

Gerald H. Lindsey, Chairman

Department of Aeronautics and Astronautics

iii

ABSTRACT

The threat of collision between an asteroid or a comet and the Earth has been well documented. Mitigation of such a threat can be accomplished by destruction of the threat or by perturbing the threat object into a safe orbit. Following a summary of proposed mitigation techniques, this thesis investigates the impulse required to safely perturb a threatening Earth-Crossing Asteroid (ECA). While previously published analysis included only two-body approximations to the impact geometry, this thesis adds the effect of the Earth's gravitational field to more closely approximate reality. The results indicate that third-body effects are strongest on ECA's in a nearly circular heliocentric orbit, where the minimum required ΔV can be several times larger than that calculated using two-body approximations. To determine the minimum ΔV required for mitigation, MATLAB®'s sequential quadratic programming (SQP) algorithm is applied to a constrained optimization problem. Third-body effects were added to a previously published two-body optimization by modifying the boundary conditions. With knowledge of the minimum ΔV requirements, the capability of current impulsive mitigation technology is analyzed. For asteroids of median density in co-planar orbits, a single 24 Mt nuclear explosive impulse applied earlier than 3 years before impact can effectively mitigate a threat with a diameter of 6 km. The capability significantly decreases with shorter warning times.

TABLE OF CONTENTS

LIST OF FIGURES

x

LIST OF TABLES

ACKNOWLEDGEMENTS

The author wants to thank Prof. I. M. Ross and Dr. S.-Y. Park for their guidance and patience during the work on this thesis.

The author would like to thank most of all his new wife and long time best friend, Carla, for her loving support and encouragement during the long hours required for the completion of this work...and for her patience during his time in Monterey.

I. INTRODUCTION

*Who knows whether, when a comet shall approach this globe to destroy it,
as it often has been and will be destroyed, men will not tear rocks from
their foundations by means of steam, and hurl mountains, as the giants are
said to have done, against the flaming mass? - And then we shall have
traditions of Titans again, and of wars with Heaven.*
                                       - Lord Byron, 1822 (Medwin, 1824, p. 185)

Although steam is no longer the motive force of choice, the defense that Lord
Byron dreamed of 150 years ago is finally possible today. For the first time in the
history of humanity, the technology exists which could potentially protect the Earth
against an impact from an asteroid or comet. In addition, the threat of impact from a
cosmic body that Lord Byron addressed has, within the last 20 years, become widely
accepted. However, while the defensive technology exists, an active planetary defense
plan does not. At this incipient stage in researching impact hazards, there are still many
challenges to be met.

Before considering the technical challenges to a defense plan, one must first
answer the question: what is the threat? Cosmic bodies in orbits that bring the
possibility of impact with the Earth are commonly termed Near Earth Objects (NEOs).
Generally, NEOs are comets or asteroids that have a perihelion radius of less than 1.3
AU. These are orbits that have the potential to be perturbed by the gravitational force of
the Earth and other planets into orbits that impact the Earth (Cheng, 1994, p. 651).

Lord Byron's quotation refers to comets, which are distinguished from asteroids
by outgassing activity or the existence of a tail (Cheng, 1994, p. 651). Comets are
believed to be composed of ice and rock (Elder, 1997, p. 11), and can approach in such
highly eccentric orbits that they can impact the Earth at velocities greater than 50 km/s
(Morrison, 1994, p. 61). The composition of asteroids varies widely from metal to the
same ice and rock found in comets (Morrison, 1994, p. 61). Because of the lower

1

eccentricity of their orbits, asteroids generally impact the Earth at velocities on the order of 20 km/s (Morrison, 1994, p. 61).

The technical challenges to a NEO defense plan can be grouped into two categories: hazard detection and hazard mitigation.

Current theory suggests that only a small percentage of all potentially hazardous Near Earth Objects (NEOs) have been discovered. It is believed that all Earth-Crossing NEOs with diameters of 6-12 km have been discovered. With smaller diameters, the detection completeness decreases dramatically: about 35% with diameters of 3-6 km, 15% with diameters from 2-4 km, and 7 % with diameters from 1-2 km. This low detection completeness implies that a significant number of objects with the potential of causing a global disaster have not yet been detected. Some specific challenges for detection are: correcting a bias in discoveries that results from the majority of searches being conducted in the Earth's northern hemisphere, improving discovery follow-up to achieve a reliable orbit calculation (Carusi, 1994, p. 145), decreasing the minimum possible detection magnitude, and coherently processing detection data (Bowell, 1994, p. 194).

Once detected, the orbital parameters of the NEO must be accurately determined. Errors in the estimation of a NEO's orbital parameters can propagate over time to produce a drastically inaccurate estimate of impact probability or time. A thorough understanding of this error propagation is critical to the planning of a defense mission. Another challenge is to model the non-gravitational effects in comets caused by rocket-like outgassing (Yoemens, 1994, p. 257) so that accurate impact probabilities can be calculated.

This thesis concentrates on some of the challenges to the mitigation of a NEO hazard. Chapter II presents a detailed study of mitigation ideas. The thesis then continues with the goal of answering two questions:

1. What is the minimum ΔV required to deflect a threat-NEO into a safe orbit?

2. What is the maximum NEO size that can be deflected with a single defense mission using current technology?

The challenges addressed in this thesis are only a fraction of those that must be overcome before a Planetary Defense system can be fielded.

II. STATEMENT OF THE PROBLEM

A. HAZARD MITIGATION TECHNIQUES

All proposed NEO hazard mitigation techniques (Simonenko, 1994; Wood, 1994; Ahrens, 1994; Solem, 1994; Canavan, 1994; Meissinger, 1995; Melosh, 1994; Shafer, 1994) attempt to accomplish one of two goals: either destroy the NEO, producing fragments that will not inflict damage if they impact the Earth, or deflect the NEO into an orbit that is no longer hazardous. Both of these techniques require a controlled coupling of energy to the NEO. Much of the analysis of hazard mitigation techniques thus far has revolved around determining the best source of energy for hazard mitigation (Canavan, 1994; Ahrens, 1994; Simonenko, 1994; Shafer, 1994; Solem, 1994; Willoughby, 1994; Melosh, 1994).

As with all space missions, the mass of the payload is a critical driver in the selection of energy source. Table 2.1 gives a comparison of the specific energies of many potential energy sources. If energy source selection were based solely on payload mass, nuclear explosive would obviously be the best choice.

High Explosive	6 MJ/kg
Kinetic Energy (10 km/s)	50 MJ/kg
Nuclear Explosive	$4*10^6$ MJ/kg

Table 2.1 Specific Energies (after Shafer, 1994)

It is instructive at this point to discuss terminology used in describing nuclear explosives. In most technical applications, the size of a nuclear explosive is expressed as the amount of energy the explosive can produce. This energy is usually measured in terms of an equivalent mass of TNT that would produce the same explosive power. Using this convention, then, 1 MT = 4.2×10^{15} Joules (Morrison, 1994, p. 61). Table 2.2 presents the mass of a nuclear explosive charge based on its yield.

5

Yield	Mass
1 Mt	0.5 ton
10 Mt	3 to 4 ton
100 Mt	20 to 25 ton

Table 2.2 Yield Versus Mass for Nuclear Explosive Devices (after Simonenko, 1994, p. 931)

However, mass is only one of several factors that must be considered in choosing an energy source. The following is a compilation of proposed NEO hazard mitigation techniques, based on the mitigation goal.

1.   Fragmentation and Dispersal

If sufficient energy is delivered to the NEO to fragment it, the hazard could be mitigated in several ways. First, differential velocities in the individual fragments of the destroyed NEO would result in a dispersed debris cloud. Some small scale fragmentation experiments suggest that if a NEO were destroyed 1 orbit prior to impact, as little as 1% of the original NEO mass would impact the Earth (Ahrens, 1994, p. 919).

The second mitigation effect of fragmenting the NEO is to reduce the size of the meteor that reaches the Earth. In order to be effective, a mitigation effort would be required to reduce the impactor size to the point that it would no longer generate damage on impact with the Earth. The atmosphere can provide a great deal of protection from some meteors, but its effects are highly dependent on the impact velocity and the composition of the NEO. Figure 2.1 shows the relation between the composition of a

6

NEO, its impact velocity, its size, and the amount of destruction that can result following atmospheric ablation and impact.
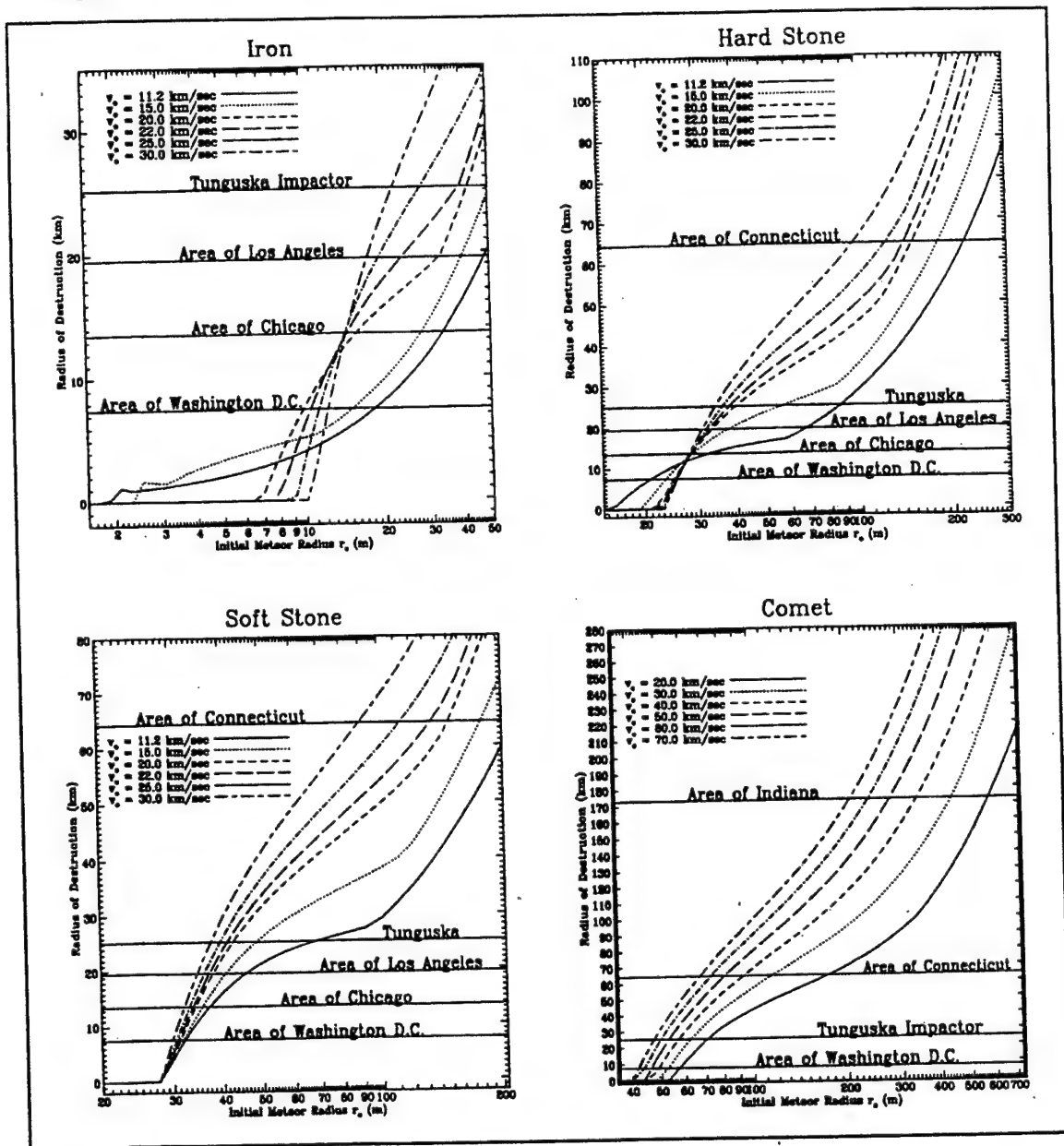
Figure 2.1 The radius of destruction around the impact point due to the atmospheric blast wave (from Hills, 1993, p. 1133).

But what is the best way to fragment the NEO? For the mass reasons discussed above, nuclear explosives are a very attractive option for the fragmentation energy source. Smaller, more loosely bound NEOs could be destroyed by a surface explosive. However,

larger and more solid NEOs would require that the explosive be buried. Burial would provide significantly greater coupling of energy to the NEO (Ahrens, 1994, p. 917).

The requirement for charge burial adds some complexity to the mitigation effort. Wood (1994) suggests some ways to effect this burial. A penetration depth of approximately 10 meters could by accomplished by use of hyper-velocity (kinetic energy) blasting prior to arrival of the nuclear charge. For larger NEOs, a string of 20-100 0.5 MT nuclear explosives could be used for penetration. Once the desired depth is achieved, a 20-300 MT charge can be directed into the void and detonated to achieve final NEO destruction.

Ahrens and Harris (1994, p. 922) estimate that a charge buried at optimal depth can destroy a hazardous NEO as summarized in Table 2.3:

NEO Diameter	Required Nuclear Explosive Yield
0.1 km	800 kg
1 km	22 Kt
10 km	0.6 Gt

Table 2.3 Nuclear Explosive Yield required to fragment hazardous NEOs (after Ahrens, 1994, p. 922)

While analysis indicates that nuclear explosives can successfully fragment a NEO, there are hazards associated with this energy source. First is the concern, presented by Meissinger (1995, p. 16), that the NEO fragments which reach the Earth following nuclear destruction could be radioactive. The most significant problem with using nuclear weapons in NEO mitigation is the tremendous political, sociological, economic, and management aspects of the weapons.

The alternatives for NEO fragmentation use the kinetic energy inherent in the closing speeds between the NEO and an interceptor. Wood (1994) proposes a "Jack-Hammer" rubblization technique in which waves of hyper-velocity projectiles are directed towards the threat object. Each projectile vaporizes a small portion of the object, leaving

8

a hole for the next projectile to enter. The cumulative effect of the impact of many projectiles is several deep holes and a somewhat fragmented NEO.

Woods' team further refines this concept (Teller, 1995) into Hypervelocity Projectile Array-Sheets and Hypervelocity Projectile Lattices. The Sheets are a two dimensional plane with multiple projectiles connected to each other. The connection helps to ensure that follow-on projectiles will be directed to impact spots of previous projectiles. The Lattice combines several Sheets into a three dimensional pulverization effort.

Thus, there are several options for fragmentation and dispersal of a threat-NEO. There are, however, arguments against using fragmentation as a mitigation goal. In order for fragmentation to significantly reduce the amount of NEO mass that eventually impacts the Earth, the NEO must be destroyed early. Thus, Ahrens and Harris conclude that "...fragmentation is likely to be a safe choice only for long lead-time response (decades) or for relatively small bodies where the fragments may be allowed to hit the Earth (Ahrens, 1994, p. 919)." If the target were pulverized late, it may make the problem worse. The resulting fragments would present multiple targets to any follow-on mitigation effort (Solem, 1994, p. 1028).

2.   Orbital Deflection

Many NEO orbital deflection schemes work by accelerating mass away from the NEO, thus changing its momentum. Chemical rockets, which have seen extensive use in space for changing the momentum of man-made satellites, are only appropriate for NEOs with diameters of less than 100 meters (Wood, 1994, p. 11). The mass of fuel required to rendezvous (by matching velocity) with the threat and then to displace it would be otherwise be excessive.

Another option is to use a mass driver. A mass driver uses electromagnetic forces to accelerate buckets containing material from the surface of the NEO (Melosh, 1994, p.

1117). Thus, a mass driver has an advantage over chemical rockets in that it avoids the need to transfer propellant mass from the Earth. While the technology for mass drivers has been available since the mid-1970's (Melosh, 1994, p. 1117), they are nonetheless very·complex. Meissinger (1995) points out that mass drivers would require large-scale, complex robotic operations for construction and processing of the NEO's soil. Also, the mass driver concept is critically dependent on the soil conditions of the NEO (Meissinger 1995). At this point, little is known about the composition or soils characteristics of asteroids and comets.

Just as the kinetic energy of the threat-NEO was used in NEO destruction schemes, there are schemes to use this kinetic energy for NEO deflection. Interestingly, for kinetic energy mitigation schemes, Canavan (Canavan, 1994, p. 102) suggests that "...the mass required scales on $\frac{m}{v^2}$, so faster NEOs present less of a threat because of their higher specific energy." In these schemes, a projectile impacts the threat-NEO and the crater ejecta combines with the momentum of the projectile to produce an impulse. Analysis conducted by Ahrens and Harris (1994, p. 904) suggests that the energy from a kinetic impact is coupled much more efficiently than the energy from nuclear weapons detonated at the surface of the NEO. Figure 2.2 shows an estimate of the capability of kinetic energy deflectors. The three lines show the capability of an impactor with a diameter of 1m, 10m, and 100m. Melosh (Melosh, 1994, p. 1115) even suggests a "billiards shot" scenario, in which a small asteroid is displaced into a larger asteroid. Wood (1994) also refines the kinetic energy approach into a "hypervelocity sand-blaster." In this scheme, a steady stream of projectiles are directed at the threat-NEO, combining their effect to produce the required momentum change.
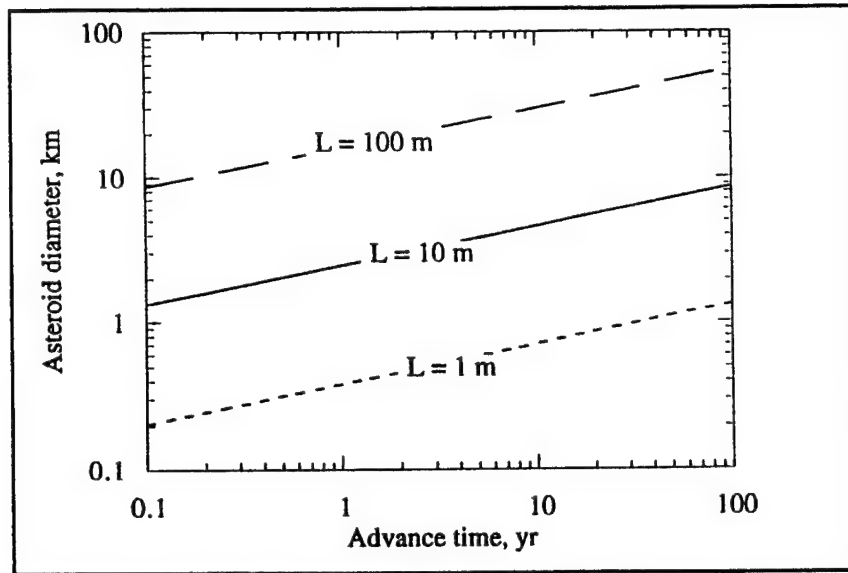
Figure 2.2 Capability of Kinetic Energy Deflectors (from Melosh, 1994, p. 1116)

The next potential technique for orbital deflection is the use of nuclear explosives.
Momentum change can be imparted on a threat-NEO using a nuclear explosive in one of
two fundamental ways: a stand-off radiative explosion or a surface explosion. For the
stand-off case, the explosive is designed to have a substantial fraction of its yield as
energetic neutrons and gamma rays. These rays irradiate the surface of the NEO that is
exposed to the explosion. The irradiated surface then expands and ablates away from the
NEO. As the material ablates away, the momentum of the NEO changes. The surface
explosion works in much the same way as a kinetic defense scheme by creating a crater.
The ejecta departing from this crater creates a momentum change in the NEO. (Ahrens,
1994, p. 910).

Not surprisingly, it is not yet clear which nuclear explosive method has the
greatest mitigation capacity. Surface nuclear explosions are generally considered more
effective in coupling energy into the NEO. Canavan (Canavan, 1994, p. 105) concludes
that "...the energy required for stand-off is greater than that for slightly subsurface bursts
by a factor of about 40." Solem (1994, p. 1032) reaches the same conclusion, stating that
a stand-off deflection would require a substantial increase in interceptor mass over a
surface burst. Ahrens and Harris (1994, p. 917), in contrast, propose that "...surface

11

explosions appear to be not substantially better than radiative stand-off explosions, in deflecting NEOs." One significant disadvantage to the surface explosion is the risk of inadvertently fragmenting the threat object. As pointed out previously, a fragmented NEO presents multiple targets for any follow-on mitigation effort. But there is fairly consistent agreement that the interceptor weight for a nuclear mitigation effort is several orders of magnitude less than that of a kinetic energy effort (Solem, 1994, p. 1032).

Lasers also have a potential use in NEO hazard defense. With this technique, a high energy laser is directed at the surface of the threat-NEO. This creates a thermal flux which ablates the surface, much like the radiative heating does in stand-off nuclear explosions. One estimate suggests that a laser output of 1 GJ/s for 12 uninterrupted days could match the energy fluence of a 1 Mt nuclear burst. (Shafer, 1994, p. 965)

Solar sails have also been proposed. Solar sails use solar radiation pressure to provide a motive force. This force is small, but consistent over long periods of time. The long build up could provide a significant change in momentum of a hazardous NEO. However, Melosh points out that "...truly enormous structures are necessary to deflect asteroids in the 1 to 10 km diameter range." Figure 2.3 demonstrates the required size. The lines are for solar sails of 10 km, 100 km, and 1000 km diameters. The technology does not yet exist to build such enormous solar sails at great distances from the Earth.
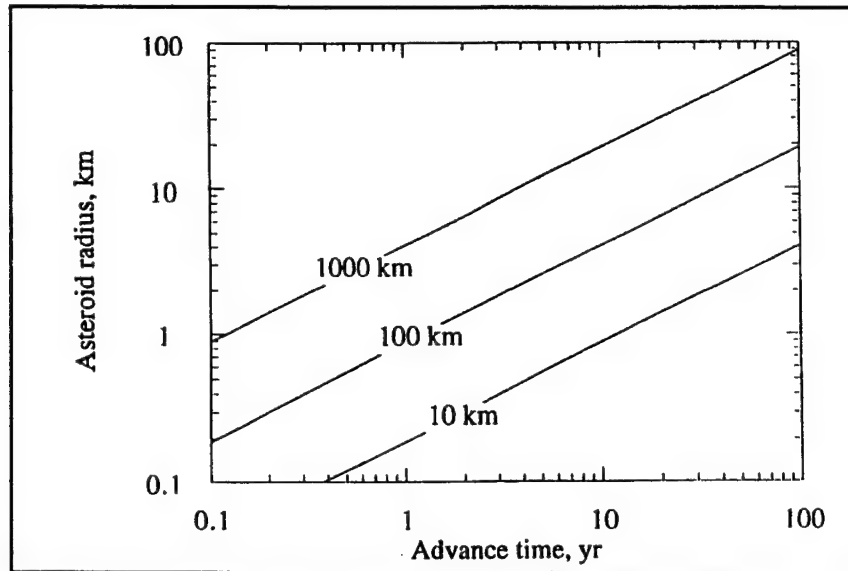
Figure 2.3 Capability of Solar Sails (from Melosh, 1994, p. 1120)

One of the more interesting non-nuclear approaches is a solar collector. Melosh

(Melosh, 1994, p. 1120) has done some extensive analysis of this approach and concludes

that, for non-nuclear alternatives, it is "...an approach that is arguably better than any

other previously proposed." This scheme also uses a solar sail, but instead of using the

solar sail directly as a motive force the sail is used to focus sunlight onto the surface of

the NEO. The surface is thus vaporized, and the ablation of surface material produces a

momentum change. Melosh indicates that a 1 km diameter solar collector, which can be

launched by the space shuttle, can deflect asteroids up to 3.4 km in diameter after

operating for a year (Melosh, 1994, p. 1125).

B.   PREVIOUS ORBITAL DEFLECTION ANALYSIS

The fundamental goal of this thesis is to investigate the effects of third-body

gravitation on orbital deflection requirements. Previous research has simplified the

problem by assuming two-body orbital mechanics between the Sun and the threat-NEO.

This assumption neglects perturbations due to the Earth's gravity. While these

perturbations may not be present until the terminal phase on the impact scenario, they

affect both long and short warning time analyses as described below.

13

1.   Long warning times

Most analyses of long warning time threats have concentrated on changing the phasing of the NEO. Ahrens (1994, p. 903) approximated the required ΔV for deflection by comparing the position of the perturbed NEO orbit with that of the unperturbed orbit. He then calculates the velocity change required to produce a displacement of 1 Earth radius ($R_{\oplus}$). Investigation of third body effects and patched conic theory indicates that a displacement of 1 $R_{\oplus}$ may be insufficient.

Earlier work done at the Naval Postgraduate School (Knudson, 1995; Park, 1997; Elder, 1997) refines the estimates of the required ΔV. All of these analyses, however, begin with a two-body approximation. One would like to know how much third-body gravitation will affect these results.

2.   Short warning times

Ahrens (1994, p. 901), Meissinger (1995), and Solem (1994, p. 1015) all assume rectilinear motion for short warning time calculations. Once again, this approximation neglects the Earth's gravitational effects, which will cause the NEO to deflect towards the Earth in a hyperbolic orbit.

A brief look at hyperbolic orbits will give an idea of how Earth's gravity will affect rectilinear approximations. When a sideways motion is imparted such that a (gravitationally free) miss distance of 1 $R_{\oplus}$ is achieved, the result is to establish a hyperbolic orbit with a semiminor axis (b) of 1 $R_{\oplus}$. Using a typical impact velocity of 20 km/s, actual perigee radius (equation from Brown, 1992, p. 27) can be calculated as follows:

$$r_p = -\frac{\mu}{V_{HE}^2} + \sqrt{\left(\frac{\mu}{V_{HE}^2}\right)^2 + b^2} = 0.856 R_{\oplus}$$

where

V_∞ = impact velocity

μ = Gravitational Constant of the Earth

Thus, preliminary approximations of energy required to deflect a threat may result in errors of 14% in miss distance, in the terminal case.

This thesis intends to further investigate the Earth's gravitational effects on energy required to defend against an impacting NEO.

III. PROBLEM FORMULATION

A. PROBLEM STATEMENT

Given a NEO with an orbit that confirms an impending collision with the Earth, and given that orbital deflection is the chosen mitigation goal, it is necessary to know the ΔV (both magnitude and direction) required to deflect the asteroid into a safe orbit. Determination of this required ΔV must include multi-body gravitational effects. A detailed understanding of third-body perturbations will help to refine previous two-body approximations.

The goal of this thesis is to investigate the effects of the Earth's gravitation on the ΔV required to deflect an Earth-impacting NEO.

B. ASSUMPTIONS

Several assumptions were made to simplify the analysis.

- The Earth and the threat-NEO are in co-planar orbits.
- The Earth is considered to be in a perfectly circular heliocentric orbit at a radius of 1 AU.
- The threat-NEO is originally in an elliptical heliocentric orbit. NEOs in hyperbolic or parabolic heliocentric orbits were not considered.
- The control maneuvers are impulsive.
- Other than the impulse, no non-gravitational forces (such as outflowing of gas and dust in comets) are included.

C. HYPERBOLIC MAPPING AND ANALYSIS

The first step was to understand how a heliocentric elliptical orbit maps into a geocentric hyperbolic orbit. The primary goal was to determine the velocity of the NEO

with respect to the Earth ($\mathbf{V}_{NEO/\oplus}$) at Earth impact. This required some vector analysis combined with orbital mechanics and geometry.

Once an equation for $\mathbf{V}_{NEO/\oplus}$ was found, an understanding of the dynamics can be aided by finding its maximum. The maximum was determined in two ways. First, Mathworks' MATLAB® was used to numerically create a 3-D plot of $\mathbf{V}_{NEO/\oplus}$ versus the NEO's heliocentric semimajor axis (a) and its heliocentric eccentricity (e). To confirm the numerical result, Warterloo's symbolic manipulator, Maple V™, was used. The original equation for $\mathbf{V}_{NEO/\oplus}$ was maximized analytically. The plot was identical to that of the MATLAB® analysis, thus verifying both analyses.

D.   PATCHED CONIC APPROXIMATION

Once the hyperbolic mapping was realized, the analysis was extended for use in a patched conic approximation. The advantage of using this approximation was that previous two-body analysis could be adapted to account for third body effects.

The most useful aspect of the patched conic approximation, for this analysis, was the B-plane and the impact radius (b_i). Figure 3.1 illustrates these parameters. The B-plane is orthogonal to the asymptote of the approach hyperbola and placed at a large distance from the Earth. The impact radius (b_i) is the semiminor axis of a hyperbola that has a perigee equal to the radius of the surface of the Earth.

18
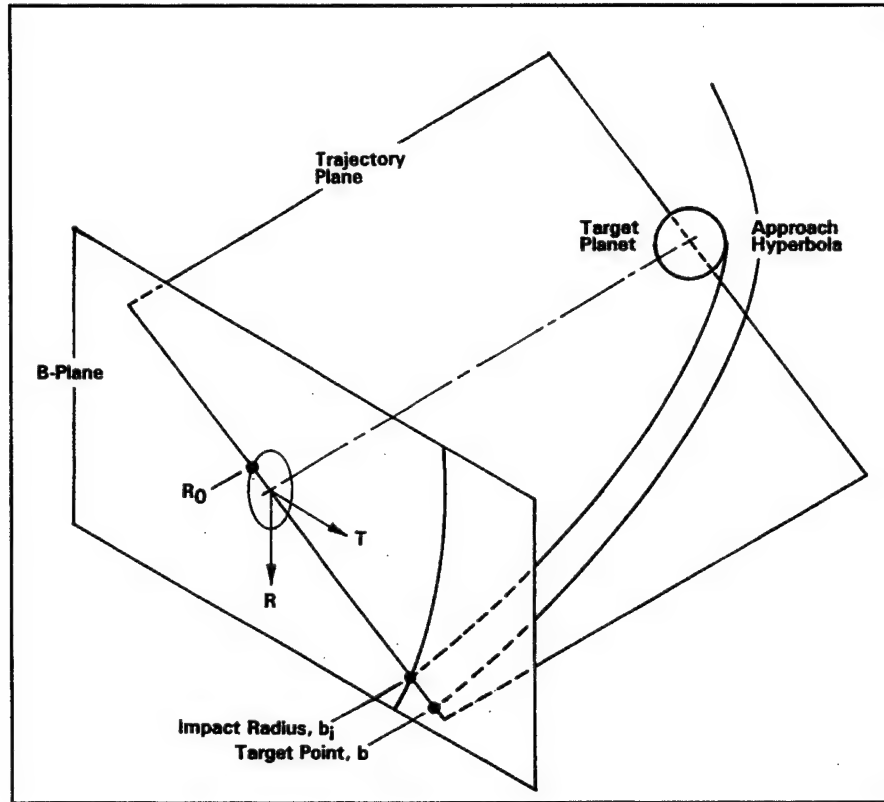
Figure 3.1 B-plane and Impact Radius (from Brown, 1992, p. 117)

The impact radius is a function of $V_{NEO/\oplus}$, which was solved for in the hyperbolic

analysis. Once this radius is determined, it can replace previous miss distances of 1 $R_\oplus$ in

two-body analysis. Thus, third-body effects are accounted for while maintaining the

relative simplicity of two-body analysis.

E. NUMERICAL TRAJECTORY OPTIMIZATION

Park, Elder, and Ross (Park, 1997) use MATLAB® 's sequential quadratic

programming method to numerically solve a constrained optimization problem to

determine the minimum ΔV for deflecting an Earth-crossing asteroid. As referred to

earlier, this code used a two-body approximation. It is possible to include the effects of

third-body gravitation in this code by adding the impact parameter in two different ways.

Discussing these modifications first requires a brief description of the code. The

code requires a target separation distance. This target separation is the minimum

19

allowable separation between the Earth and the perturbed NEO. Following an impulse, the Earth's orbit and the NEO's orbit are propagated using the two-body equations of motion to determine the minimum separation. The optimization problem minimizes the impulse by equalizing the propagated and the target separations.

The first modification of the code is to increase the target separation distance. If this target separation is increased to a minimum impact radius in the B-plane, then the Earth's gravity will not cause an impact.

Second, the constraints of the optimization problem can be modified. In its original form, the constraints require that the minimum separation equal some fixed distance. With the first modification, this fixed distance is the impact radius of the NEO's original orbit. Once the NEO's orbit changes (after application of the ΔV), there is a new impact radius. If this new impact radius is larger than the original impact radius, the NEO will still impact the Earth. The solution is to modify the constraint to include the impact radius directly. This modification requires that the minimum separation be equal to the impact radius.

IV. HYPERBOLIC ORBIT ANALYSIS

A. CONIC SECTIONS

Orbits in an inverse square gravitational field take the shape of conic sections: circular, elliptical, parabolic, or hyperbolic. Circular orbits are a special case of the elliptical orbit. These two types of orbits are defined when the object's energy is insufficient to escape the gravitational attraction of the central mass. The parabolic orbit is a transition between elliptical and hyperbolic orbits. An object passing a central mass on a parabolic trajectory would reach an infinite distance from the mass, but with zero velocity. Any object with a velocity less than that of a parabolic orbit will not escape the central mass, and thus will be in an elliptical orbit. Conversely, an object with a greater energy than that of a parabolic orbit will escape the central mass. When the object is traveling faster than this escape velocity, it is in a hyperbolic orbit.

B. ELLIPTICAL ORBITS

Before they become a threat to Earth, nearly all NEOs are established in an elliptical orbit about the Sun. Figure 4.1 shows the geometry of an elliptical orbit.
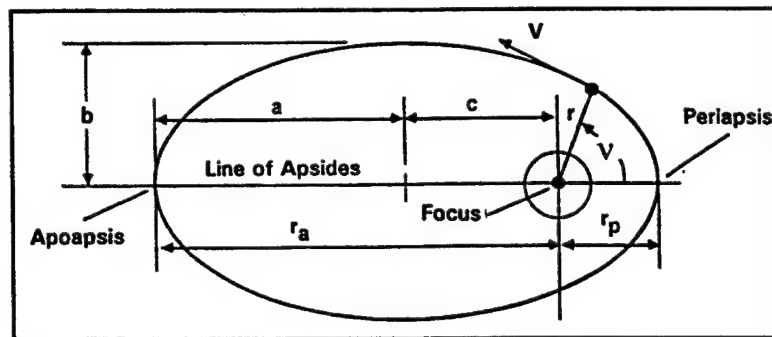
Figure 4.1 Elliptical Orbit (after Brown, 1992, p. 9)

For the two-dimensional case considered in this thesis, only the semi-major axis (a), eccentricity (e), and true anomaly (v) are required to define an orbit and position.

a = semimajor axis, the distance from the center of the ellipse to the long edge

e = eccentricity, defines the shape of the orbit ($0 \leq e < 1$ for an elliptical orbit)

υ = true anomaly, defines the position within the orbit

The most important elliptical orbit relation required for this analysis is the NEO's heliocentric velocity as it reaches the orbit of the Earth. This velocity is given by (Brown, 1992, p. 19)

$$V = \sqrt{\frac{2\mu}{r} - \frac{\mu}{a}} \qquad (4.1)$$

Also useful is the distance of the NEO from the Sun as a function of the true anomaly, given by (Brown, 1992, p. 18)

$$r = \frac{a(1 - e^2)}{1 + e\cos\upsilon} \qquad (4.2)$$

C.   HYPERBOLIC ORBITS

In an impact scenario, a NEO which was in an elliptical orbit about the Sun will transition, as it approaches the Earth, to a hyperbolic orbit about the Earth. An understanding of hyperbolic orbits, and this transition, is therefore fundamental to studies of the orbital mechanics of NEO impacts.

The orbital parameters of a hyperbolic orbit, shown graphically in Figure 4.2, are similar to the familiar elliptical orbit parameters (Brown, 1992, p. 21):

r_p = periapsis radius

a = absolute magnitude of the semimajor axis, the distance from the asymptote focus to the periapsis

b = semiminor axis, distance from the asymptote to a parallel passing through the central body

c = the distance from the asymptote focus to the center of mass

e = eccentricity = c/a (greater than 1 for hyperbolic orbit)

β = angle of the asymptote

θ_a = true anomaly of the asymptote
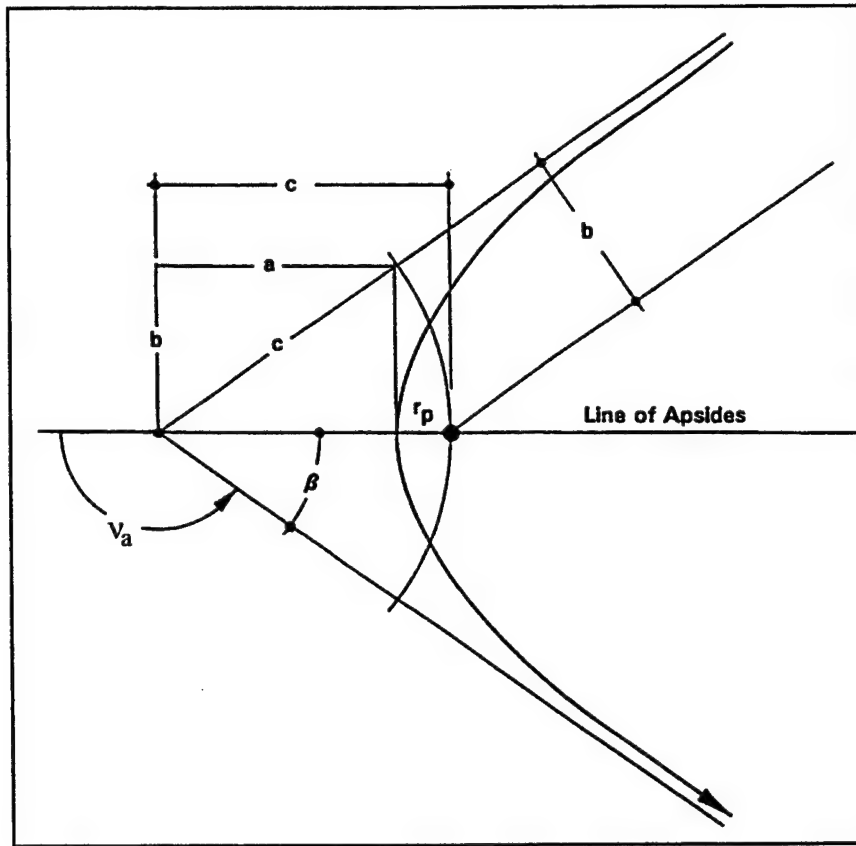
Figure 4.2 Elements of a hyperbola (after Brown, 1992, p. 22)

All of the orbital parameters of a hyperbolic orbit can be determined with a knowledge of two parameters: the velocity at an infinite distance from the central mass (V_∞) and the semiminor axis (b). From knowledge of V_∞, the semimajor axis can be calculated by the relation (Brown, 1992, p. 28)

$$V_\infty = \sqrt{\frac{\mu}{a}} \tag{4.3}$$

Once the semimajor axis (a) is determined, the eccentricity can be calculated by (Brown, 1992, p. 27)

$$e = \sqrt{1 + \frac{b^2}{a^2}} \tag{4.4}$$

Periapsis radius (r_p) is expressed as (Brown, 1992, p. 27)

23

$$r_p = -\frac{\mu}{V_\infty^2} + \sqrt{\left(\frac{\mu}{V_\infty^2}\right)^2 + b^2} \qquad (4.5)$$

And finally, the angle of the asymptote (β) is (Brown, 1992, p. 27)

$$\tan \beta = \frac{b}{a} \qquad (4.6)$$

D. PATCHED CONIC METHOD

The patched conic method was originally developed to simplify the planning of interplanetary trajectories, yet it applies directly to analysis of NEO impacts on the Earth.

Each celestial body, due to its mass, generates a gravitational field which affects all other celestial bodies according to Newton's Laws of motion and gravity (Wiesel, 1997, p. 35)

$$m_i \ddot{\mathbf{r}}_i = \sum_{j \neq i}^{N} \frac{G m_i m_j}{r_{ij}^2} \frac{\mathbf{r}_j - \mathbf{r}_i}{r_{ij}} \qquad (4.7)$$

This is known as the N-body problem. An exact solution for more than two bodies does not exist (Weisel, 1997, p. 35). However, the patched conic method makes some minor approximations that reduce the N-body problem to solvable two-body problems.

The patched conic method assumes that an object is influenced by the gravitational field of a planet only when it is within the planet's "sphere of influence." Beyond the sphere of influence, the object is considered to only be affected by the Sun's gravitation. The radius of the sphere of influence is somewhat nebulous, but Laplace suggests (Brown, 1992, p. 97),

$$R_{SOI} \approx R \left(\frac{M_{planet}}{M_{sun}}\right)^{2/5} \qquad (4.8)$$

where

R_{SOI} = radius of the sphere of influence of the planet

R = mean orbital radius of the planet

M_{planet} = mass of the planet

M_{Sun} = mass of the Sun

For Earth, this equates to a sphere of influence of 0.9×10^6 km.

In the case of a NEO impact scenario, the NEO begins in an elliptical orbit about the Sun. Once within the sphere of influence of the Earth, the NEO's motion is described by two-body orbit equations for a hyperbolic orbit about the Earth.

E.   DETERMINING V_∞

To define the orbit of the NEO as it approaches the Earth, it is necessary to determine V_∞. Figure 4.3 shows the vector geometry of an impact scenario, where:

$\mathbf{V}_{NEO/\odot}$ = the velocity of the NEO with respect to the Sun

$\mathbf{V}_{\oplus/\odot}$ = the velocity of the Earth with respect to the Sun

$\mathbf{V}_{NEO/\oplus}$ = the velocity of the NEO with respect to the Earth, defined as $\mathbf{V}_\infty$ in this

thesis

Strictly speaking, $\mathbf{V}_{NEO/\oplus} \neq \mathbf{V}_\infty$, because the NEO is not at infinity with respect to the Earth. However, in the patched conic method the approximation is made as $\mathbf{V}_{NEO/\oplus} \approx \mathbf{V}_\infty$.
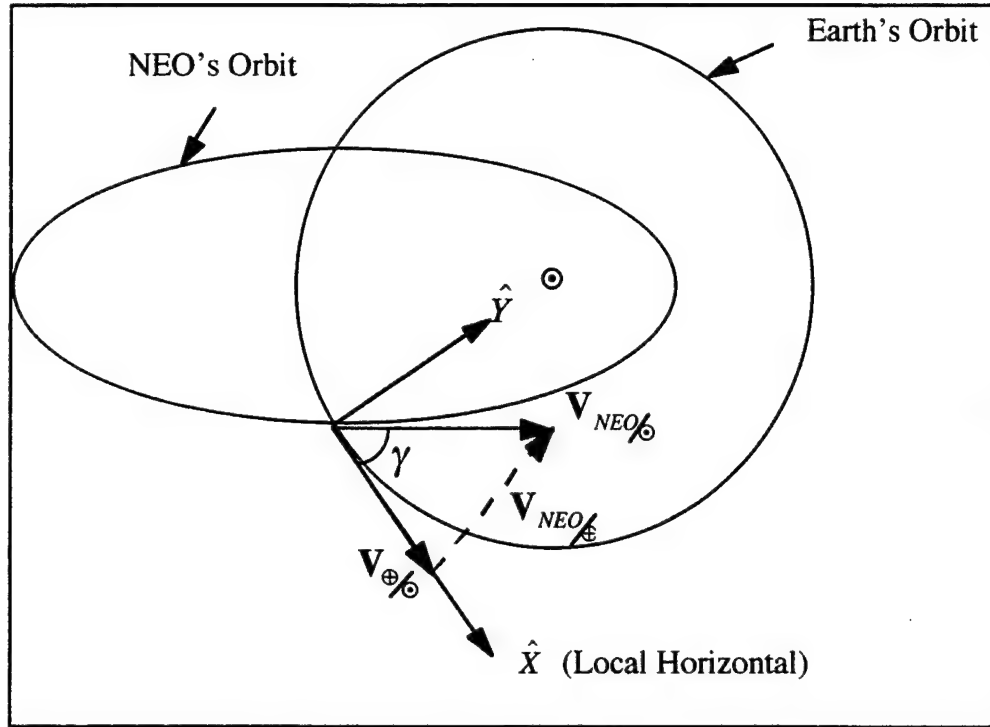
Figure 4.3 Vector Geometry at Impact

Using vector algebra, $\mathbf{V}_\infty$ can be expressed as:

$$\mathbf{V}_{\oplus/\odot} + \mathbf{V}_{NEO/\oplus} = \mathbf{V}_{NEO/\odot} \tag{4.9}$$

$$\mathbf{V}_{NEO/\oplus} \equiv \mathbf{V}_\infty = \mathbf{V}_{NEO/\odot} - \mathbf{V}_{\oplus/\odot} \tag{4.10}$$

The velocity of the Earth with respect to the Sun ($\mathbf{V}_{\oplus/\odot}$) can be determined at any

time, using the equation for velocity in a circular orbit

$$\mathbf{V}_{\oplus/\odot} = \sqrt{\frac{\mu_\odot}{r_{\oplus/\odot}}}\hat{\mathbf{X}} \tag{4.11}$$

with

$r_{\oplus/\odot}$ = the distance of the Earth from the Sun = 1 AU

To find the other unknown, $\mathbf{V}_{NEO/\odot}$, some approximations are required. The

radius of the sphere of influence is very small in comparison to the radius of the Earth's

orbit about the Sun. Thus, calculating the velocity of the NEO as it crosses the Earth's

orbit is a very close approximation to the velocity as it crosses the Earth's sphere of

influence (SOI). In the worst case geometry, this approximation introduces an error in radius of

$$\frac{r_{SOI}}{r_{\oplus/\odot}} \times 100\% = \frac{0.9 \times 10^6 \, km}{1.496 \times 10^8 \, km} \times 100\% = 0.6\% \tag{4.12}$$

Strictly speaking, this approximation changes equations 4.9 and 4.10 from equalities to approximations.

Now the magnitude of $\mathbf{V}_{NEO/\odot}$ is calculated by

$$V_{NEO/\odot} = \sqrt{\frac{2\mu_\odot}{r_{\oplus/\odot}} - \frac{\mu_\odot}{a_{NEO/\odot}}} \tag{4.13}$$

with

a = the semimajor axis of the NEO with respect to the Sun

For the direction of $\mathbf{V}_{NEO/\odot}$, the flight path angle (γ) is required. The flight path angle is a function of the position of the object within its orbit. This position is defined by the true anomaly (υ), shown in Figure 4.4. In an impact scenario with a known NEO orbit, the true anomaly at impact can be calculated as follows (where $e :=$ the eccentricity of the NEO's heliocentric orbit):

$$\left(r_{NEO/\odot}\right)_{IMPACT} = r_{\oplus/\odot} = \frac{a\left(1-e^2\right)}{1 + e\cos\left(\upsilon_{NEO/\odot}\right)_{IMPACT}} \tag{4.14}$$

After manipulation, Equation 4.14 yields

$$\left(\upsilon_{NEO/\odot}\right)_{IMPACT} = \cos^{-1}\left[\frac{a\left(1-e^2\right)}{er_{\oplus/\odot}} - \frac{1}{e}\right] \tag{4.15}$$
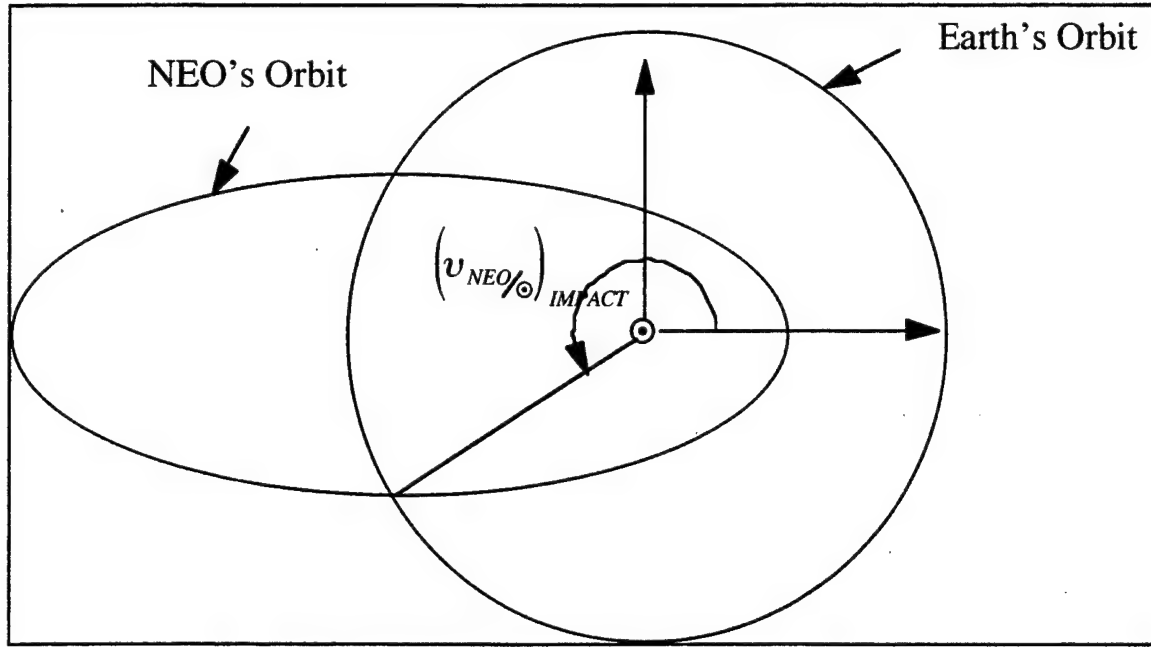
Figure 4.4 Definition of true anomaly

Given the position of the NEO and it's heliocentric eccentricity, the flight path angle is calculated by (Brown, 1992, p. 18)

$$\tan\gamma = \frac{e\sin\upsilon_{NEO/\odot}}{1+e\cos\upsilon_{NEO/\odot}} \tag{4.16}$$

Thus Equations 4.13, 4.15, and 4.16 combine to give both the magnitude and direction of $\mathbf{V}_{NEO/\odot}$. Returning to Equation 4.10, $\mathbf{V}_\infty$ can finally be determined:

$$\mathbf{V}_\infty = \mathbf{V}_{NEO/\odot} - \mathbf{V}_{\oplus/\odot} \tag{4.10}$$

$$\mathbf{V}_\infty = \left(V_{NEO/\odot}\cos\gamma\;\hat{\mathbf{X}} + V_{NEO/\odot}\sin\gamma\hat{\mathbf{Y}}\right) - V_{\oplus/\odot}\hat{\mathbf{X}} \tag{4.17}$$

$$\boxed{\begin{aligned} \mathbf{V}_\infty &= \left(\sqrt{\frac{2\mu_\odot}{r_{\oplus/\odot}} - \frac{\mu_\odot}{a}}\cos\gamma - \sqrt{\frac{\mu_\odot}{r_{\oplus/\odot}}}\right)\hat{\mathbf{X}} + \left(\sqrt{\frac{2\mu_\odot}{r_{\oplus/\odot}} - \frac{\mu_\odot}{a}}\sin\gamma\right)\hat{\mathbf{Y}} \\[2mm] \tan\gamma &= \frac{e\sin\upsilon_{NEO/\odot}}{1+e\cos\upsilon_{NEO/\odot}} \\[2mm] \left(\upsilon_{NEO/\odot}\right)_{IMPACT} &= \cos^{-1}\left[\frac{a\left(1-e^2\right)}{er_{\oplus/\odot}} - \frac{1}{e}\right] \end{aligned}} \tag{4.18}$$

Equations 4.18 are an important result. Although they look complicated, it is apparent that V_∞ is a function of only two variables: the NEO's heliocentric eccentricity (e) and semimajor axis (a). The flight path angle and radius are set by the geometry of the impact. Since the Earth is assumed to be in a circular orbit, and the problem is planar, this geometry is defined by the NEO's orbit.

F.   MAXIMUM V_∞

As previously discussed, V_∞ is a critical value in defining the hyperbolic orbit of the NEO about the Earth's center of gravity. Now that V_∞ has been directly related to e and a, a better understanding of this relation can be achieved by attempting to find its maximum.

1.   Variable Bounds

If it is possible to find bounds for each parameter in equations 4.16, it may be possible to determine a maximum V_∞. Such a study will potentially provide an insight into the full geometry of the problem.

To determine a value for the minimum semimajor axis of the NEO (a_{min}), recall that

$$a = \frac{r_a + r_p}{2} \qquad (4.19)$$

A minimum value for the NEO's semimajor axis is mandated by the fact that the orbit must intersect the Earth's orbit for an impact to occur. This sets the value of r_a to the radius of the Earth's orbit. The NEO also cannot have a perihelion radius less than the radius of the Sun ($R_\odot$). Thus, a_{min} is defined by

$$a_{min} = \frac{r_{\oplus/\odot} + R_\odot}{2} \qquad (4.20)$$

The maximum value of the semimajor axis is infinite. This is because the aphelion radius is unbounded, although the perihelion radius cannot be larger than the radius of the Earth's orbit. This becomes more clear when using the following elliptical relation

$$a = \frac{r_p}{1-e} \tag{4.21}$$

In an impact scenario with a NEO in an elliptical heliocentric orbit, the eccentricity varies as $0 \le e < 1$. Thus, as the eccentricity approaches 1, the semimajor axis approaches infinity. The bounds of the semimajor axis can be summarized as follows:

$$\boxed{\frac{r_{\oplus/\odot} + R_\odot}{2} \le a < \infty} \tag{4.22}$$

The bounds of the NEO's eccentricity are set by the initial assumption that the NEO is in an elliptical heliocentric orbit. Expressed mathematically,

$$\boxed{0 \le e < 1} \tag{4.23}$$

The NEO's true anomaly at impact ($\left(\upsilon_{NEO/\odot}\right)_{IMPACT}$) is fixed by the NEO's orbit. If this orbit crosses the Earth's orbit at perihelion, $\left(\upsilon_{NEO/\odot}\right)_{IMPACT} = 0$. If, on the other hand, impact occurs at the NEO's aphelion, $\left(\upsilon_{NEO/\odot}\right)_{IMPACT} = \pi$ radians. In between these two extremes, the impact can happen at one of two separate true anomalies. Figure 4.4 (above) demonstrates this fact. Thus, the true anomaly at impact in bounded as follows (expressed in radians):

$$\boxed{0 \le \left(\upsilon_{NEO/\odot}\right)_{IMPACT} < 2\pi} \tag{4.24}$$

To understand the bounds of the flight path angle (γ), a graph of the relation between flight path angle and true anomaly is useful. This graph is presented in Figure 4.5.
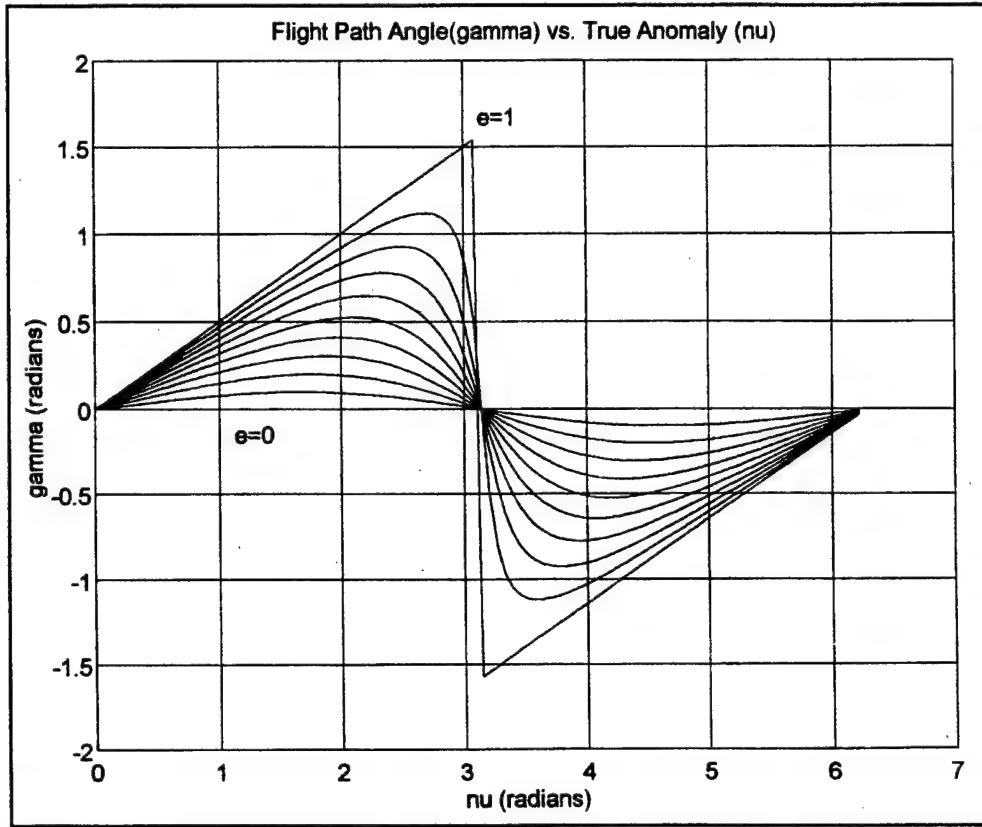
Figure 4.5 Flight Path Angle of the NEO at impact relative to True Anomaly for various eccentricities

One can see from the figure that the flight path angle varies between $-\dfrac{\pi}{2}$ and $\dfrac{\pi}{2}$.

$$\boxed{-\frac{\pi}{2} < \gamma < \frac{\pi}{2}}$$ (4.25)

In conclusion, a study of the bounds of each parameter does not readily reveal a relation for V_∞. Thus, a plot of V_∞ may be more helpful.

2.   Graphical Display

Since V_∞ is a function of only two variables, it is possible to generate a three-dimensional plot of V_∞ against e and a. A small MATLAB m-file was written to generate such a plot. The m-file is listed in Appendix A. The plot is displayed in Figure 4.6.
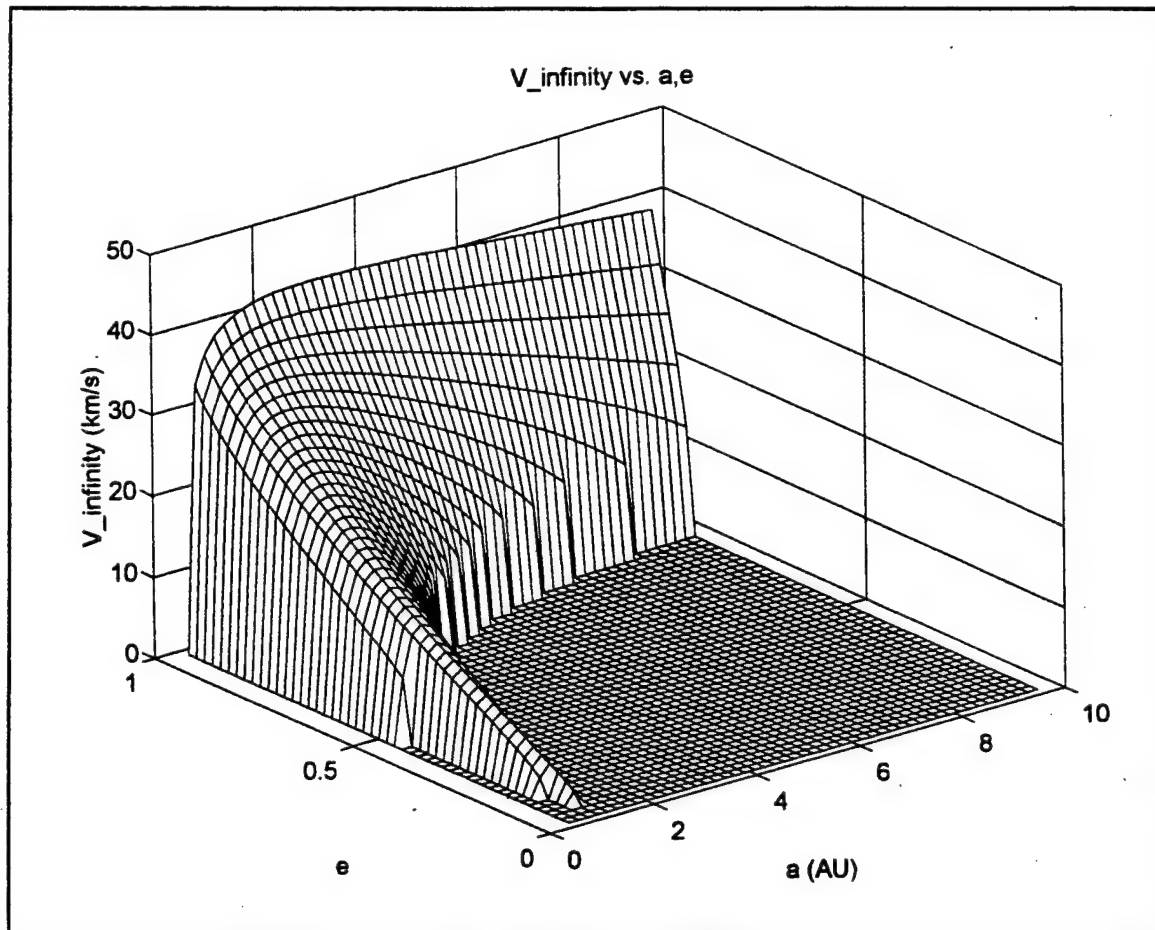
Figure 4.6 V_∞ as a function of NEO eccentricity and semimajor axis

The flat portion of this graph represents NEO orbits that do not intersect the Earth's orbit. Note that for a given NEO eccentricity there is a semimajor axis that generates the maximum V_∞. This is demonstrated graphically by the plot in Figure 4.7.
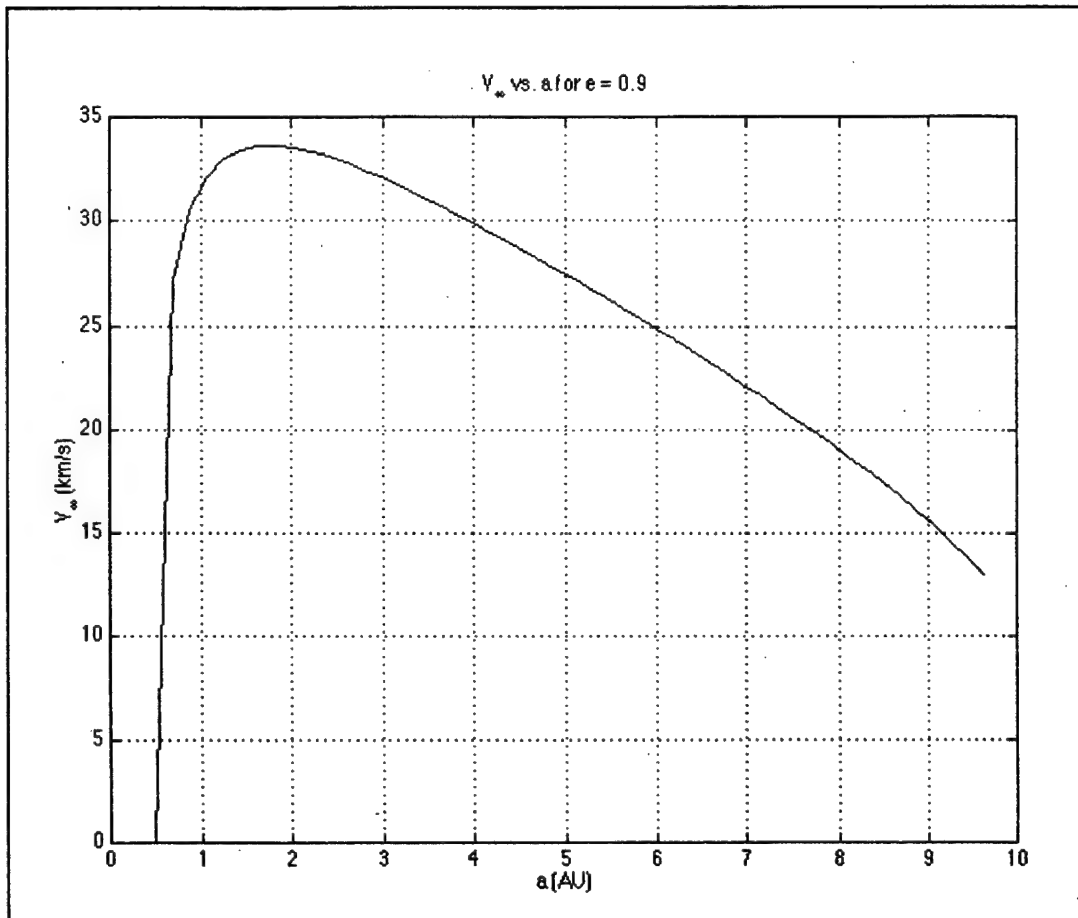
Figure 4.7 Variation of V_∞ for a fixed NEO eccentricity

A second effect apparent in Figure 4.7 is the increase in V_∞ as the NEO's eccentricity increases.

3. Closed Form Solution

As a final attempt to understand the geometry that defines V_∞, the symbolic manipulator Maple V™ was used to generate a closed form solution for the maximum value for V_∞. The Maple V™ code is included in Appendix B.

The first step in the effort to find a closed form solution is to combine all of Equations 4.18 into one equation. Because of the assumption that the NEO is in an elliptical orbit about the Sun, it is possible to reduce the Maple V™ solution to the following equation:

$$
\mathbf{V}_\infty(a,e) = \left[\frac{-\sqrt{-\dfrac{\mu_\odot a\left(r_{\oplus/\odot} - 2a\right)}{r_{\oplus/\odot}}} + e^2\sqrt{-\dfrac{\mu_\odot a\left(r_{\oplus/\odot} - 2a\right)}{r_{\oplus/\odot}}} - \sqrt{\mu_\odot\left(e^2 - 1\right)\left(r_{\oplus/\odot} - 2a\right)}}{\sqrt{r_{\oplus/\odot}\left(r_{\oplus/\odot} - 2a\right)\left(e^2 - 1\right)}} \right]\hat{\mathbf{X}}
$$

$$
+ \left[-\frac{\sqrt{-a\left(ae^2 + r_{\oplus/\odot}^2 - 2ar_{\oplus/\odot} + a^2\right)\left(r_{\oplus/\odot} - 2a\right)^2 \mu_\odot}}{a\left(r_{\oplus/\odot} - 2a\right)r_{\oplus/\odot}} \right]\hat{\mathbf{Y}}
$$

(4.26)

Next, the square of the magnitude of the velocity was calculated by adding the square of both components of the vector in Equation 4.26. In order to simplify the expression for the location of maximum V_∞, the function was left as the square of the magnitude. By eliminating the square root, the expression is simplified, but the final result will be the same. After simplification, the magnitude of V_∞ reduces to

$$
V_\infty^2 = \frac{-\left\{ \mu_\odot r_{\oplus/\odot}^3 + 6\mu_\odot r_{\oplus/\odot} a^2 + a\left[-5\mu_\odot r_{\oplus/\odot}^2 + 2\sqrt{-(e-1)(e+1)\left(r_{\oplus/\odot} - 2a\right)^2 \mu_\odot^2 r_{\oplus/\odot} a} \right] \right\}}{r_{\oplus/\odot}^2 a\left(r_{\oplus/\odot} - 2a\right)}
$$

(4.27)

Since the plots in the last section show that there is a semimajor axis (a) for each eccentricity (e) which generates a maximum V_∞, it will be most instructive to find an expression for maximum V_∞ with a fixed eccentricity. Thus, Equation 4.27 is differentiated with respect to the semimajor axis, with the eccentricity held constant. This derivative reduces to

34

$$\frac{\left[\mu_\odot r_{\oplus/\odot}\, a^2(e^2-1)+r_{\oplus/\odot}\sqrt{-(e-1)(e+1)\left(r_{\oplus/\odot}-2a\right)^2\mu_\odot^2 r_{\oplus/\odot}\, a-2\mu_\odot a^3 e^2+2\mu_\odot a^3}\,\right]\mu_\odot}{r_{\oplus/\odot}\, a^2\sqrt{-(e-1)(e+1)\left(r_{\oplus/\odot}-2a\right)^2\mu_\odot^2 r_{\oplus/\odot}\, a}}=0$$

(4.28)

Solving Equation 4.28 for the semimajor axis gives

$$a=\frac{r_{\oplus/\odot}\sqrt[3]{-\left(e^2-1\right)^2}}{e^2-1}$$

(4.29)

This relatively simple equation, considering the complexity of the derivation, is an important result. The equation determines the semimajor axis that will generate the maximum V_∞ for a given eccentricity.

Mathematically, there is no guarantee that Equation 4.29 is a maximum. Since only one derivative has been performed, all that is known is that Equation 4.29 is an extremum. In the Maple V™ procedure, inputting Equation 4.29 into the second derivative produced a very complicated result. Analysis of this result did not confirm that Equation 4.29 was a maximum. However, an eccentricity of 0.9 gave a semimajor axis of 1.739, which matches the maximum of the plot in Figure 4.7. This confirms that Equation 4.29 matches the graphical result and yields a maximum..

G.   MAPPING TO A GEOCENTRIC ORBIT

As stated before, two parameters are required to define a hyperbolic orbit: V_∞ and the semiminor axis (b). The last sections went into great detail about determining V_∞. However, knowledge of the NEO's heliocentric orbit is insufficient to uniquely fix the geocentric semiminor axis.

In order to fix the semiminor axis, one would require exact knowledge of the location of the NEO, with respect to the Earth, as it crosses the Earth's sphere of influence. All that is known about the impact problem is the NEO's heliocentric orbital

35

parameters, and the prediction of a future impact with Earth. Knowledge of the heliocentric orbit only fixes the NEO's V_∞ as it crosses the sphere of influence. However, there is no single semiminor axis that will define an impact based on V_∞.

A parameter used in the patched conic approximation for interplanetary arrival targeting can be applied directly to the impact problem. This parameter will determine a minimum semimajor axis required to avoid impact. The definition of this parameter is first based on the B-plane. Shown in Figure 3.1, the B-plane is perpendicular to the asymptote of the approach hyperbola, and placed at an infinite distance from the Earth (Brown, 1992, p. 116).

In this Figure the semiminor axis (b) is a radius, drawn in the B-plane, from the location that the NEO pierces the B-plane to a line perpendicular to the B-plane that intersects the center of mass of the Earth. The impact radius (b_i) is the semiminor axis that defines a hyperbolic orbit which is tangent to the surface of the Earth. Whenever the NEO passes inside the impact radius, it will impact the Earth. Thus, the impact radius defines a minimum safe semiminor axis. The impact radius is a function of V_∞ and can be calculated from the general hyperbolic relation (Brown, 1992, p. 28)

$$b = r_p \sqrt{\frac{2\mu}{r_p V_\infty^2} + 1} \qquad (4.30)$$

For the impact radius specifically about the Earth,

$$b_i = R_\oplus \sqrt{\frac{2\mu_\oplus}{R_\oplus V_\infty^2} + 1} \qquad (4.31)$$

Since the previous analysis determined V_∞ as a function of the NEO's heliocentric orbital parameters, it is now possible to define the Impact Radius as a function of the NEO's orbital parameters. A plot of this relation is included in Figure 4.8.
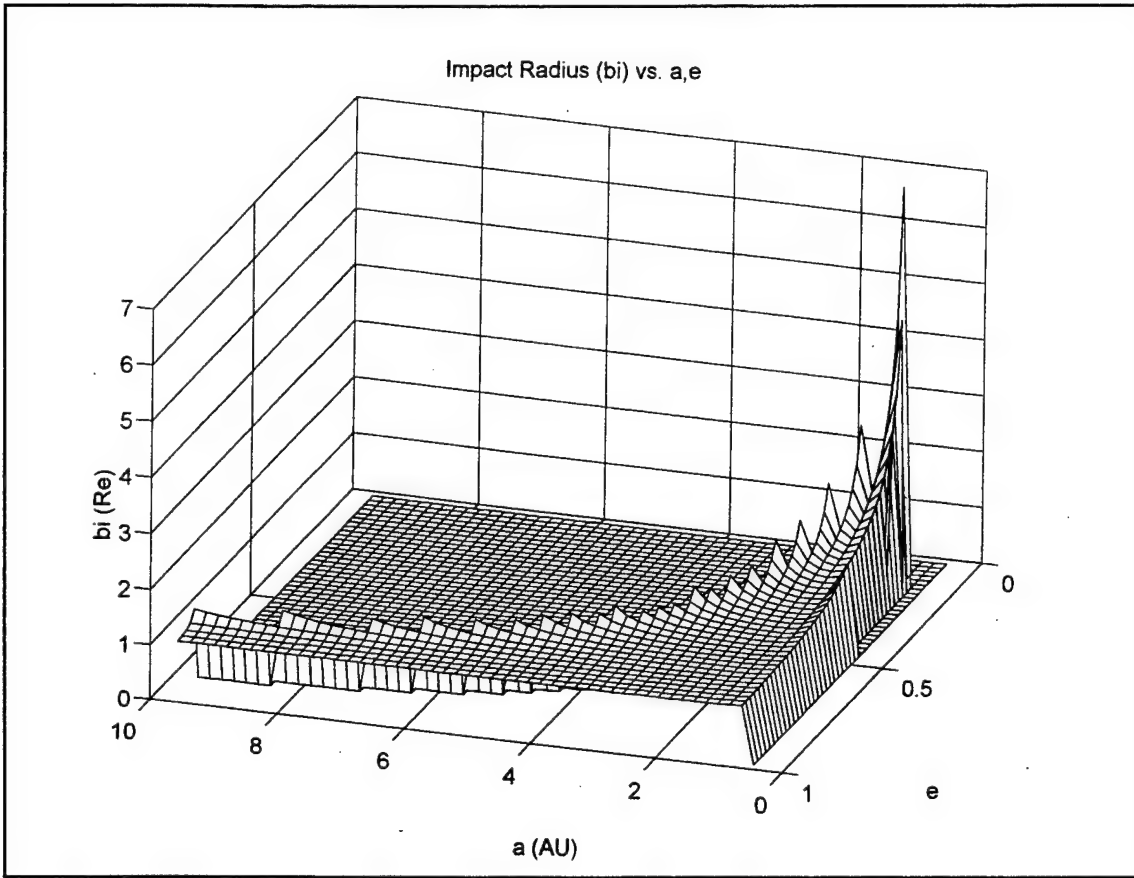
Figure 4.8 Impact Radius as a function of the NEO's eccentricity and semimajor axis

Note that, for clarity, the axes have been rotated from those used in Figure 4.6.

Figure 4.8 confirms an important conclusion that can be reached from study of Equation 4.31: the impact radius increases significantly as V_∞ decreases. This is an important result when extended to analysis of the NEO impact problem. Hence, the greatest error in previous analysis (Knudson, 1995; Park, 1997; Elder, 1997; Ahrens 1994; Meissinger, 1995; Solem, 1994) which neglected third-body effects arises when the NEO's orbit defines a small V_∞. These orbits are nearly circular, and close to the Earth (that is, with a ~ 1 AU).

V.   APPLICATION OF THE PATCHED CONIC APPROXIMATION

The preceding chapter established a theoretical foundation for applying a patched conic approximation to a three-body analysis of NEO hazard mitigation. Using this approach, a two-body analysis can be modified to include third-body effects.

In their paper entitled "Minimum Delta-V For Deflecting Earth-Crossing Asteroids," Park, Elder, and Ross (Park, 1997) presented a trajectory optimization problem that was solved numerically using a sequential quadratic programming (SQP) method. The goal of the code was to determine an optimal ΔV to deflect an asteroid, but it did so using only a two-body approximation. The patched conic approximation has since been added to the code. The results are presented here.

A.   ORIGINAL TRAJECTORY OPTIMIZATION PROBLEM

The performance index chosen to minimize ΔV is

$$J = \sqrt{\Delta V_{\parallel}^2 + \Delta V_{\perp}^2} \tag{5.1}$$

where $\Delta V_{\parallel}$ is the component of ΔV which is parallel to the motion of the object and $\Delta V_{\perp}$ is the component perpendicular to the motion. The constraints consist of the two-body equations that govern the motion of the NEO and the Earth about the Sun. Three terminal boundary conditions are set by the desired minimum miss distance. First, the miss distance at the final time must be equal to the minimum miss distance. Expressed mathematically

$$R - R_{critical} = 0 \tag{5.2}$$

where R is the distance between the Earth and the NEO and $R_{critical}$ is the proposed miss distance from the Earth. The two additional boundary conditions come from the requirement that R be at a minimum when it reaches $R_{critical}$. Because R is continous and differentiable, this can be expressed as

$$\dot{R} = 0 \tag{5.3}$$

$$\ddot{R} \geq 0 \tag{5.4}$$

B.   THIRD BODY MODIFICATIONS TO THE ORIGINAL PROBLEM

Third body effects can be added to the original formulation by modifying the boundary conditions in one of two ways. Both modifications are new definitions for $R_{critical}$ as used in Equation 5.2.

In the first modification, $R_{critical}$ is redefined to be equal to the impact radius (in the B-plane) of the original NEO orbit. Once the original orbital parameters of the impacting NEO are determined, the user can input the desired miss distance and the modified code computes the impact radius as a function of the original NEO parameters. This can be expressed mathematically as

$$R - b_i\left(a_{NEO, origianl}, e_{NEO, original}, separation\right) = 0 \tag{5.5}$$

where "separation" is the desired minimum separation between the NEO and the center of mass of the Earth.

The second modification defines $R_{critical}$ as the impact radius of the NEO orbit after perturbation. Instead of defining $R_{critical}$ based on the original NEO orbital parameters, this modification recalculates the impact radius after the perturbation is applied and confirms that $R_{critical}$ is still equal to the impact radius. The second modification therefore changes the boundary condition to

$$R - b_i(a, e, separation) = 0 \tag{5.6}$$

The two modifications produced slightly different results. The first modification changed only one calculation of b_i and thus had little effect on the run time for the code. The second modification required several calculations of b_i during execution of the code and thus increased the run time significantly. However, Equation 5.6 is a more direct statement of the required miss distance. This equation accounts for the fact that the

impulse which diverts the NEO will generate a new orbit. Since the impact radius is a function of the NEO's orbit, the perturbation will also generate a new impact radius. Equation 5.6 thus ensures that even the perturbed NEO will not pass within the impact radius. All results discussed below refer to the third-body modification expressed in Equation 5.6.

C.   SQP NON-LINEAR OPTIMIZATION ALGORITHM

The trajectory optimization code written by Dr. Park is called Earth Defense against Asteroid Impact (EDAI).

From the user's viewpoint, the code flows according to the diagram in Figure 5.1.
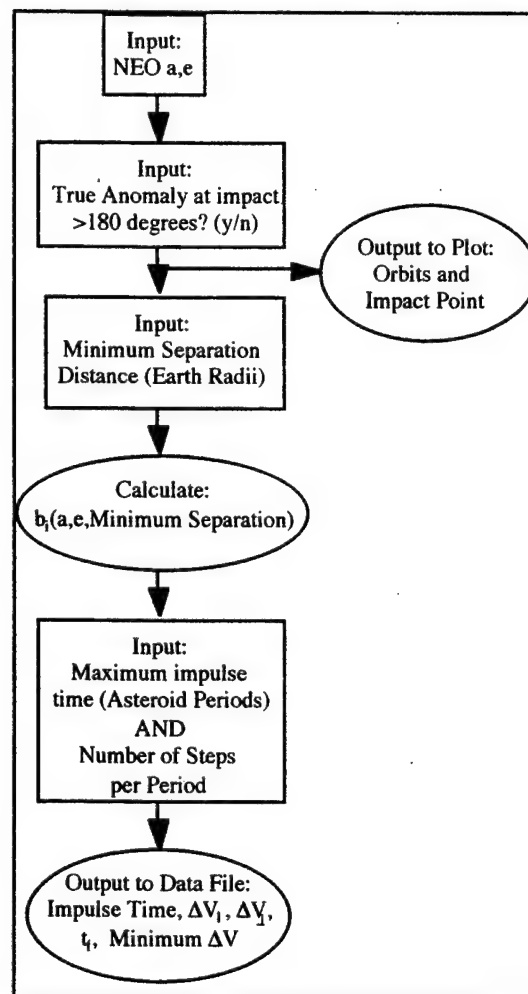
Figure 5.1 EDAI Flow Diagram

41

At this early stage in the development of EDAI, the user is required to be very knowledgeable about the code's design. There are several parameters that must be adjusted, within the code, before each run. With some adjustments, discussed in the concluding chapter, the code can be much more user-friendly.

As with all numerical optimization programs, the EDAI code is somewhat unstable with bad initial guesses. A critical parameter in the code is the initial guess of the minimum ΔV. If this initial guess is significantly different from the true value, the numerical optimization can become unstable, as is typical with numerical codes. Currently, there is no way to change this initial guess without getting into the code. Thus, if the user wishes to initialize a new EDAI run with NEO orbital parameters that are different from the previous run, he must input an accurate initial guess into the code. The initial guesses used for this analysis are included in Appendix C.

Another instability comes from round-off error when trying to achieve a minimum separation of one Earth radius. Since the code uses AU as the distance unit, a minimum separation of 1 $R_\oplus$ is extremely small. This is easily solved, due to the linearity of the problem, by running the code with a larger minimum separation (e.g., 10 $R_\oplus$) and dividing the result to achieve the desired separation (e.g., divide by 10).

The results of each run are saved in a file which is named within the EDAI code. This technique allows for many kinds of analysis of the results. However, in order to change the file name one must make a modification directly to the code.

D.   RESULTS OF THIRD BODY MODIFICATIONS

The impact radius (b_i) is highly dependent on the orbital parameters of the NEO, as displayed in Figure 4.9. Since the third body modifications to the EDAI code make use of the impact radius, the differences in results are also highly dependent on the NEO's orbital parameters.

42

First, consider NEOs with a nearly circular orbit (e close to zero). In this case, the impact radius is relatively large. Thus, one would expect the difference between the results of the 2-body model and the 3-body model to be relatively large. Figure 5.2 is a plot of the minimum ΔV required to generate a 1 $R_\oplus$ miss, as calculated by both the 2-body and 3-body codes, for a nearly circular orbit. (Note that, for standardization, all results will be presented at 1 $R_\oplus$ minimum separation.) The x-axis is the time that the impulse is applied, in units of NEO periods before impact with the Earth. The y-axis is the minimum ΔV required in units of cm/s.

Park (Park, 1997, p. 6) presents a thorough explanation of the results of the EDAI code. In summary, there are two effects apparent in the results. The first order variation in minimum ΔV required is dependent on the change in orbital elements of the NEO after perturbation. The second order variation shows local minima at the perihelion of the NEO orbit. These extrema demonstrate the commonly known effect that a ΔV applied at the perihelion has a greater efficiency in changing an orbit than when applied at any other place.
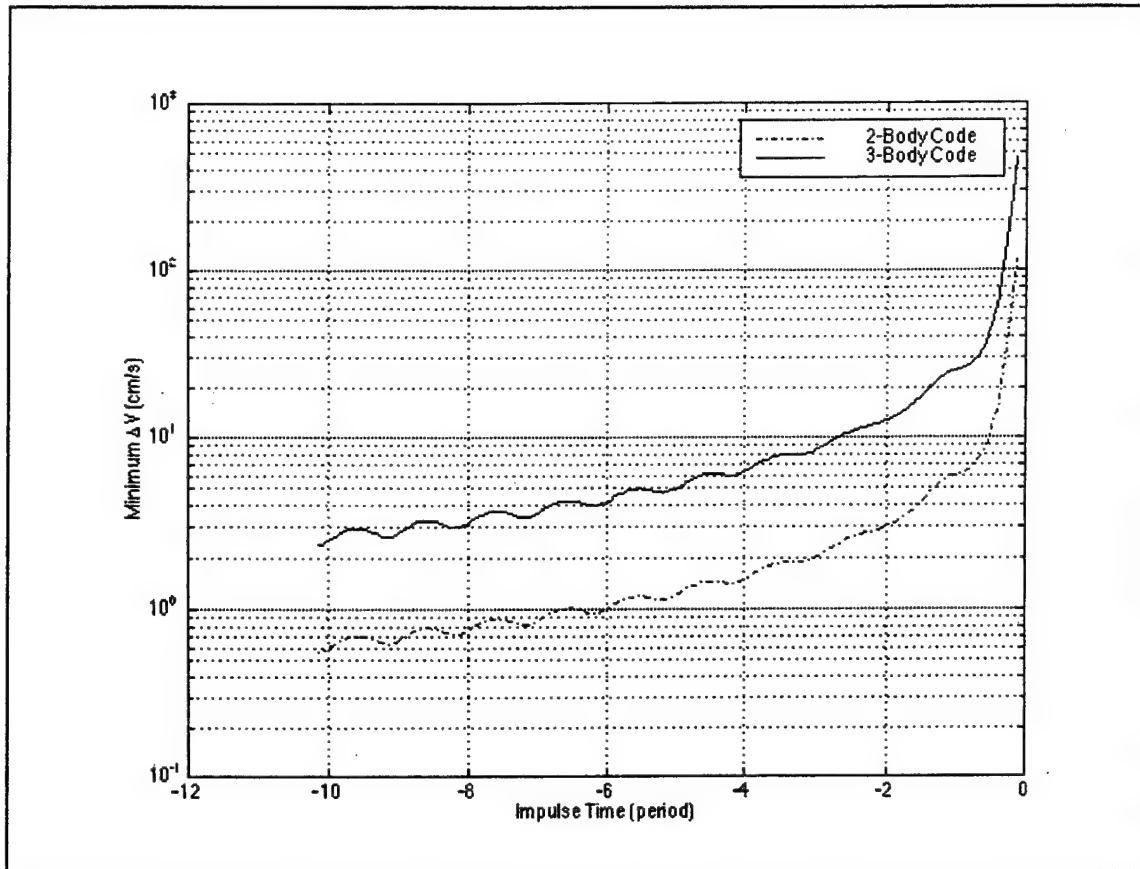
Figure 5.2 Minimum ΔV for 1 $R_\oplus$ Separation (e=0.1, a=1.05 AU)

For the original NEO orbit used in the plot for Figure 5.2, the impact radius is 4.192 $R_\oplus$. Figure 5.3 shows that when the results of the three-body analysis are divided by the results of the two-body analysis the answer oscillates about a factor of approximately 4.195. This oscillation could be identical to the variation in the impact radius for various impulse times. However, this hypothesis has not yet been verified. Verification is suggested in the recommendations for future work.
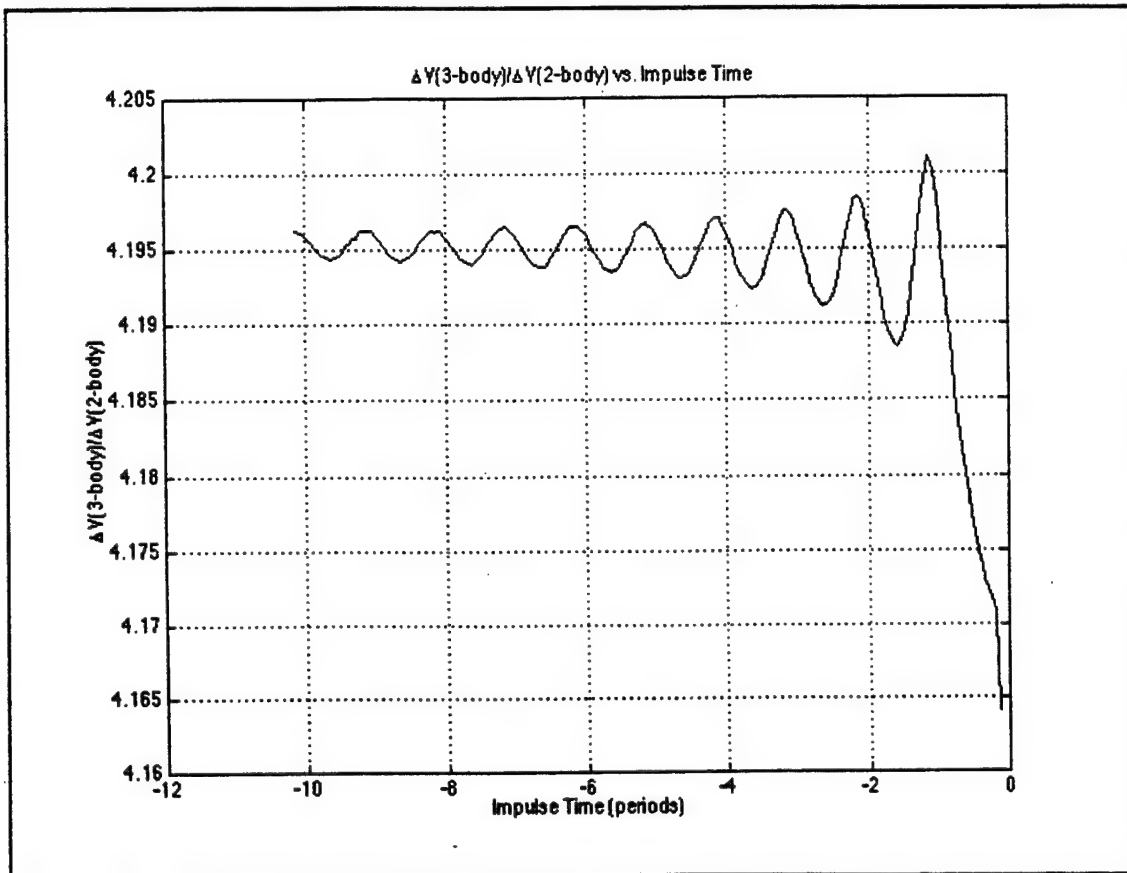
Figure 5.3 ΔV(3-body)/ΔV(2-body) (e=0.1, a=1.05 AU)

Figure 5.4 plots the difference between the 3-body and the 2-body models. The critical information in this plot is the increasing effect of the Earth's gravity as the impulse time decreases. This demonstrates the need to include the Earth's gravity in planning for short warning deflection scenarios. By not including this effect, the required minimum ΔV can be in error by more than an order of magnitude.

45
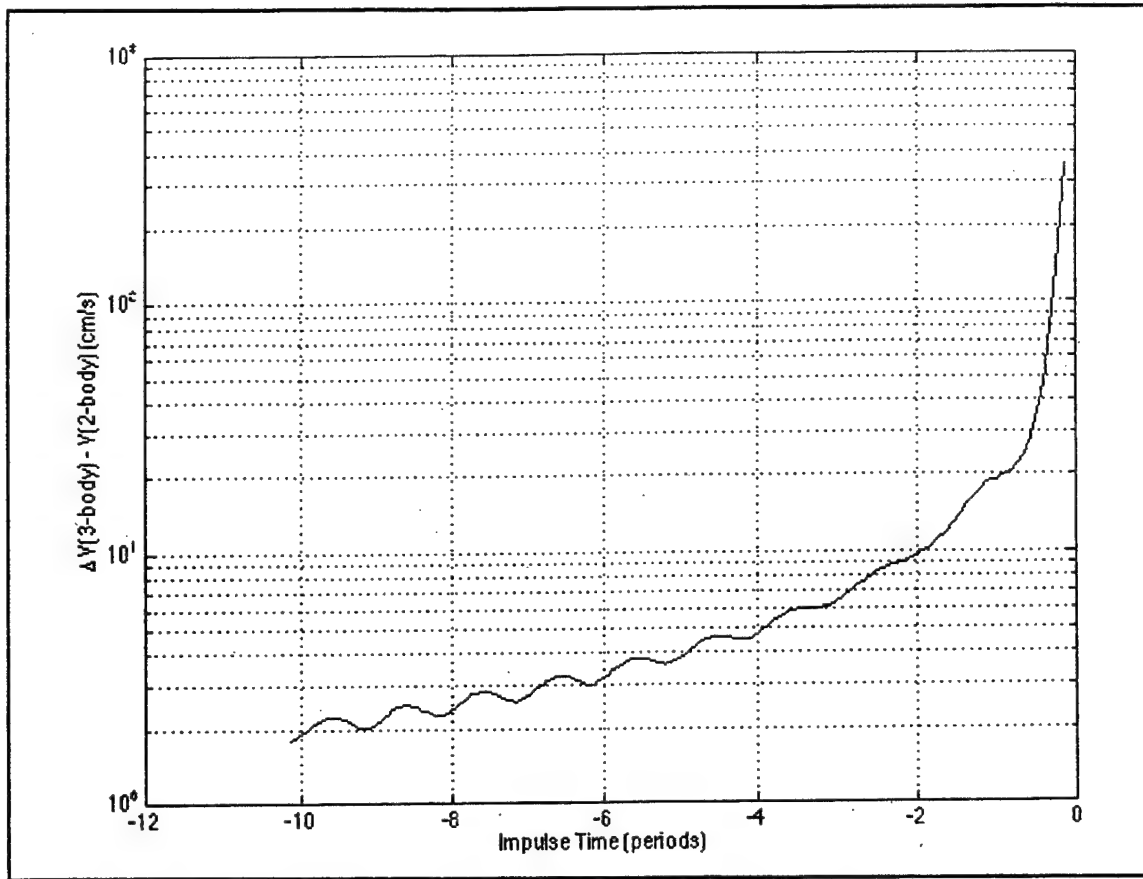
Figure 5.4 Difference Between 3-Body and 2-Body models (e=0.1, a=1.05 AU)

Referring once again to Figure 4.9, it is apparent that the impact radius for highly eccentric NEOs is nearly one. Thus, one would expect that adding third body effects to the analysis of such NEOs would have little effect. Figure 5.5 is a plot of the minimum ΔV required for a NEO with eccentricity increased to e=0.9 and the semi-major axis remaining at a=1.05 AU. While it is nearly impossible to tell, both the 2-body and 3-body results are included in the plot. This very close correlation is a result of the fact that the impact radius for this original NEO orbit is 1.0593 $R_\oplus$.
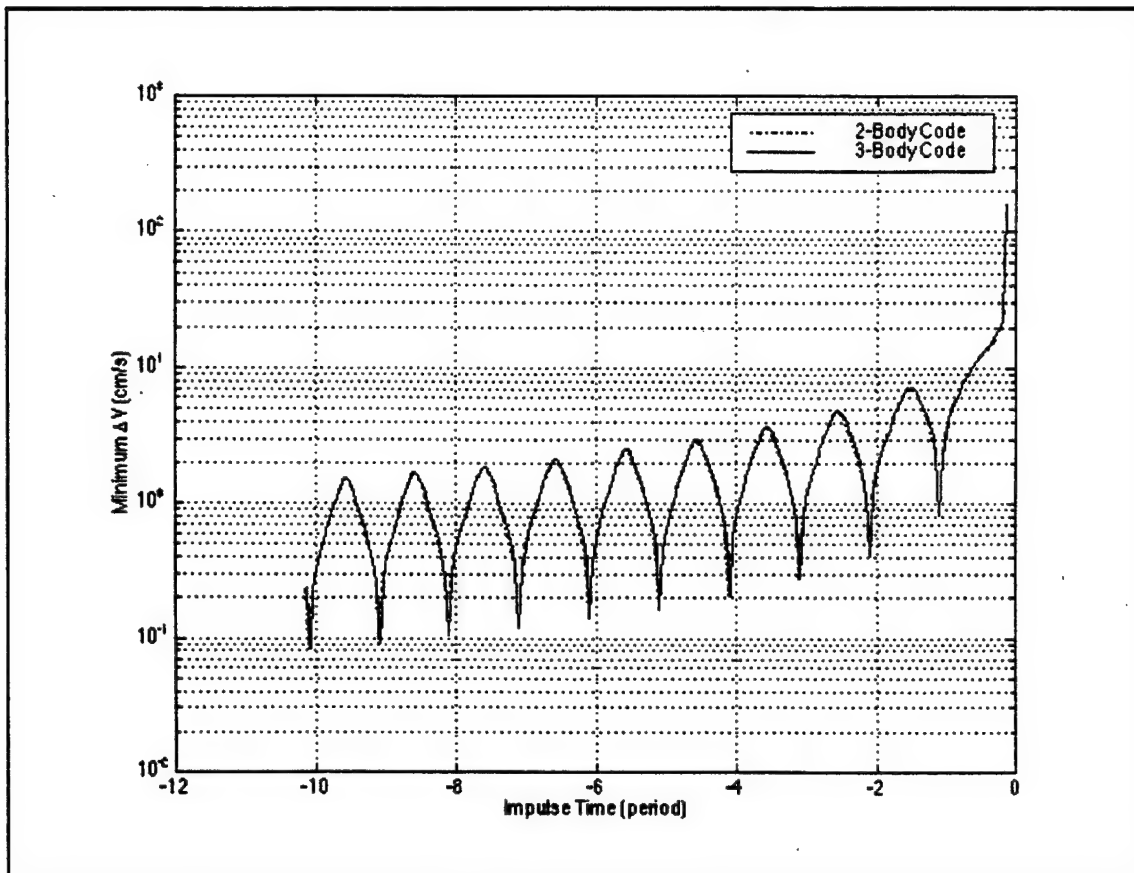
Figure 5.5   Minimum ΔV for 1 $R_\oplus$ Separation (e=0.9, a=1.05 AU)

While the effects of the third-body modification are significantly smaller than with the nearly circular orbit, the trends are the same with both NEO orbits. Figure 5.6 shows that the error increases with decreasing impulse time, just as in the first orbit.
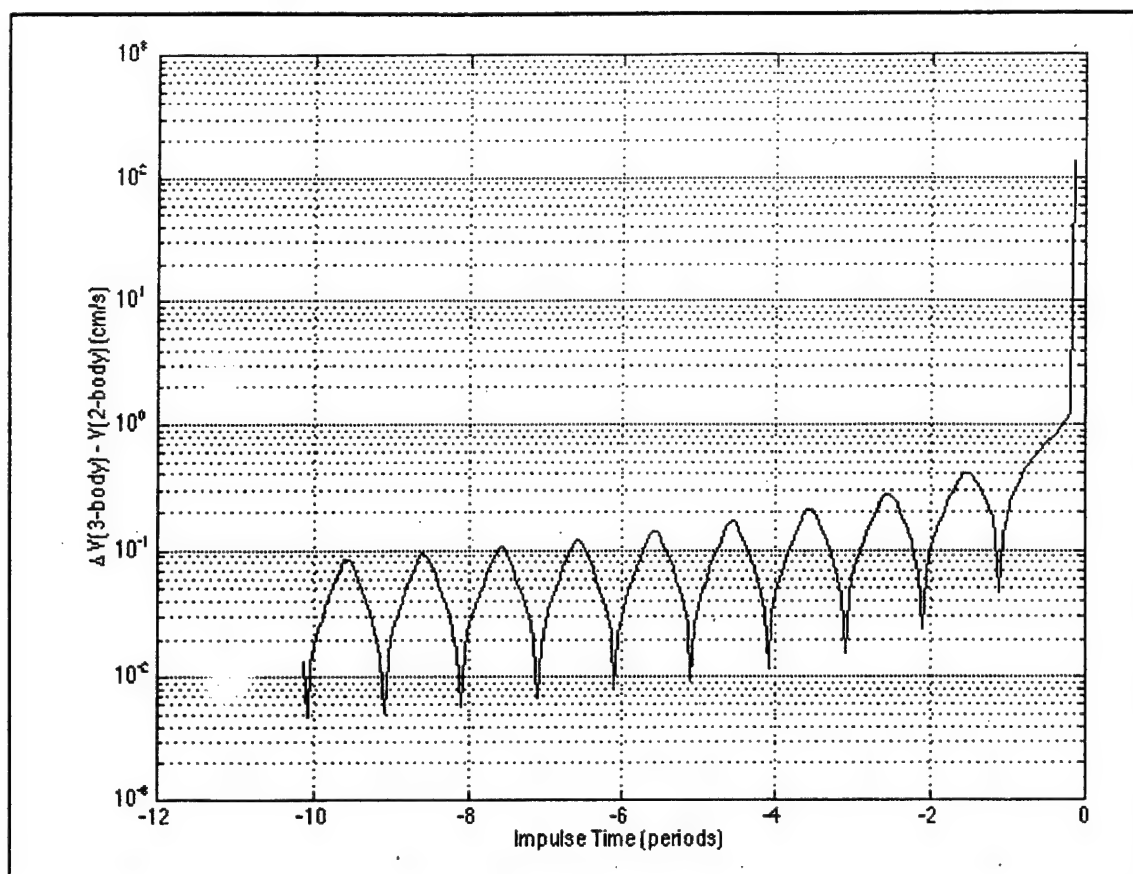
Figure 5.6   Difference Between 3-Body and 2-Body models (e=0.9, a=1.05 AU)

A critical benefit from adding the third body effects to the code is that the short warning results are now much more accurate. The final two plots are details of the minimum ΔV results for the two orbits for the timeframe of less than one orbital period. Note the sharp variation in the plot in Figure 5.8. The variation occurs when the NEO is near perihelion. As in the subsequent passes through perihelion, the ΔV requirement to perturb the NEO into a safe orbit is minimum at perihelion. Figure 5.8 shows that this applies during short warning time scenarios as well.
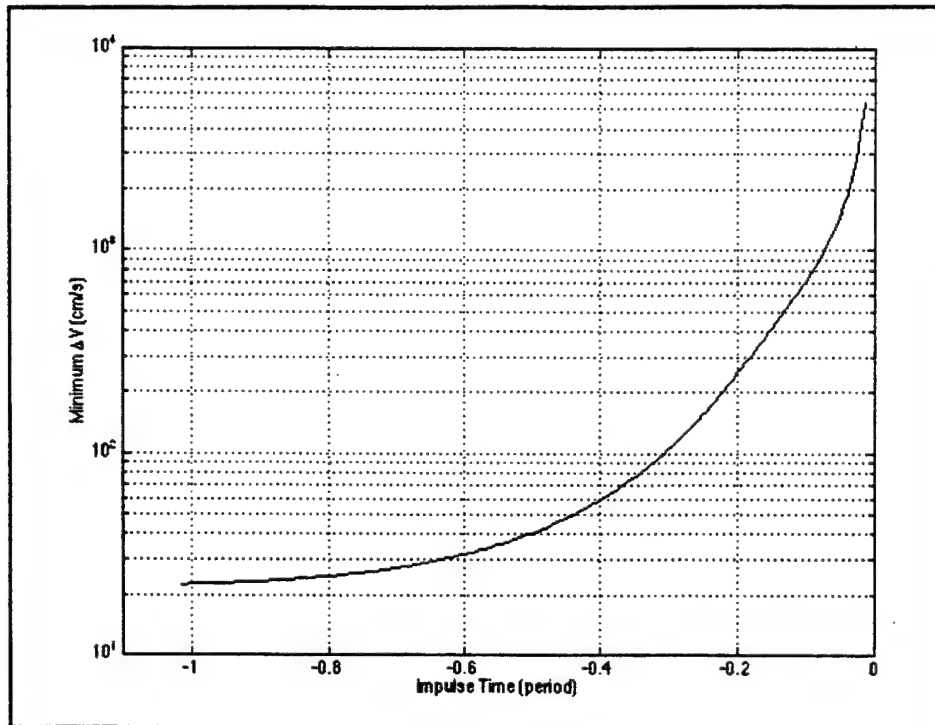
Figure 5.7 Short Warning Minimum ΔV for 1 $R_{\oplus}$ Separation (e=0.1, a=1.05 AU)
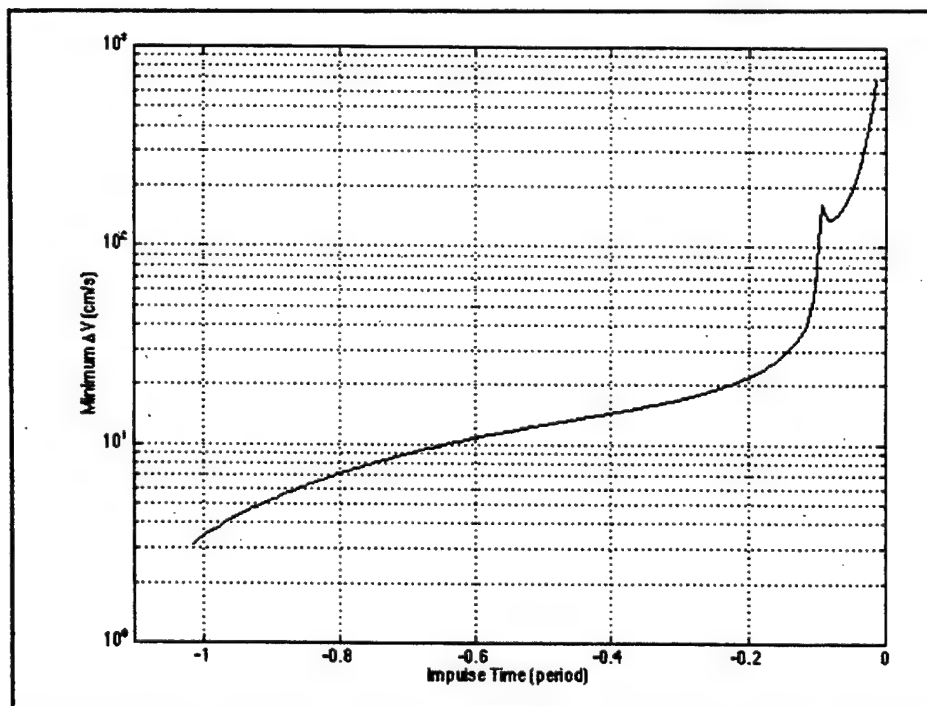
Figure 5.8 Short Warning Minimum ΔV for 1 $R_{\oplus}$ Separation (e=0.9, a=1.05 AU)

49

VI. MITIGATION CAPABILITY OF CURRENT IMPULSE TECHNOLOGIES

With a high degree of confidence in the new three-body minimum ΔV results, it is now possible to evaluate the potential of current technologies for deflection of NEOs. While Chapter II presented several ideas with potential for NEO deflection, the three-body analysis of this thesis was based on an assumption of an instantaneous ΔV (that is, an impulse). An impulse is practically impossible, and the only three methods discussed which approximate an impulse are kinetic impactors, a stand-off nuclear blast, and a surface nuclear blast.

There are many variables to consider when analyzing the capability of an impulse technology, including the physical properties of the NEO, the mass and closing velocity of a kinetic impactor, or the explosive yield and stand-off distance of a nuclear interceptor. Ahrens and Harris (Ahrens, 1994, p. 897) present a detailed analysis of the effects of these variables. This analysis was combined with the minimum ΔV results from the last chapter to evaluate current deflection capabilities.

A. KINETIC IMPACT

A kinetic impactor imparts a ΔV on a NEO by the exchange of momentum from the collision of the impactor's mass and by creating a crater. The ejecta from the crater accelerates away from the NEO, thus causing a change in momentum.

In their analysis, Ahrens and Harris obtain an expression for the mass ratio between the kinetic impactor (M_i) and the NEO (M_{NEO}) as follows.(Ahrens, 1994, p. 906)

$$\frac{M_i}{M_{NEO}} \approx \frac{\Delta v}{v_i} \bigg/ \left[1 + 0.16\left(\frac{\rho}{\rho_i}\right)\left(\frac{\rho v_i^2}{Y}\right)^{0.209} \right] \qquad (6.1)$$

where

Δv = change in NEO velocity

51

v_i = impact speed

ρ = NEO density

ρ_i = kinetic impactor density

Y = NEO material strength

The numerator of Equation 6.1 gives the ΔV resulting from an inelastic collision, while the denominator accounts for the added momentum change from the crater ejecta.

It should be noted that Ahrens and Harris differentiate between two different regimes in their analysis. For smaller NEOs, the strength of the NEO dominates the cratering mechanism. This effect is referred to as the strength regime. The gravity regime applies to larger NEOs where gravitational effects dominate cratering (Ahrens, 1994, p. 904). The results were not significantly different, so the strength regime is used for the current analysis.

B.   STAND-OFF NUCLEAR BLAST

A stand-off nuclear blast can impart a ΔV on a NEO by heating its surface until it expands and ablates away from the NEO. The ablated material is mass accelerating away from the NEO, thus causing a momentum change. Ahrens and Harris (Ahrens, 1994, p. 912) conclude that the effect of a stand-off nuclear blast can be expressed as

$$\Delta v \approx 0.1 \frac{nAW}{D^3} \tag{6.2}$$

with

n = efficiency of neutron production

A = Geometrical efficiency factor (accounts for stand-off distance)

W = nuclear explosive yield (expressed in Kt)

D = NEO diameter (in km)

Equation 6.1 expresses the NEO size in terms of mass, while Equation 6.2 uses diameter. For consistency, and for more direct application in the MATLAB m-file, Equation 6.2 was modified to give

$$M_{NEO} \approx \frac{0.1nAW\rho\pi}{6\Delta v} \qquad (6.3)$$

C. SURFACE NUCLEAR BLAST

The mechanism for momentum change with a surface nuclear blast is nearly identical to that of the kinetic impactor, except that the increased energy of the nuclear explosive creates a significantly larger crater. Since there is little experimental data about the effects of nuclear cratering in the strength regime, Ahrens and Harris present only a rough but educated estimate. The effect of a surface nuclear blast is therefore approximated by (Ahrens, 1994, p. 913)

$$W \approx 4e - 5\Delta v M_{NEO} \qquad (6.4)$$

where Δv is expressed in cm/s and M_{NEO} in kg.

D. ASSUMPTIONS

Several assumptions are required in the analysis of mitigation technology capabilities. The physical properties of the NEO required by Equations 6.1 and 6.3 are the yield strength (Y) and the density. The yield strength can vary from 10^7 dyne/cm^2 for soft rock or ice to 10^9 dyne/cm^2 for hard rock (Ahrens, 1994, p. 906). For this analysis, a value of 10^8 dyne/cm^2 was used. The density of asteroids ranges from $2x10^3$ kg/m^3 to $5x10^3$ kg/m^3 with a mean density of $3x10^3$ kg/m^3 (Elder, 1997, p. 10). Comets are somewhat less dense than asteroids, with estimates of 1000 to 2000 kg/m^3 (Elder, 1997, p. 10). A mean asteroid density of $3x10^3$ kg/m^3 was used for this analysis.

Assumptions are also required for the mitigation technology. The goal of this analysis is to determine the maximum NEO size that can be diverted using a single mission with today's technology. It is always possible to send multiple diversion missions against a NEO threat, but a single mission baseline gives the most fundamental result. Rustan (Rustan, 1994, p. 1070) presents a summary of launch vehicle

performance which includes the useful payload that can be place on an interplanetary trajectory. He indicates that the Russian Energia vehicle can place a payload mass of 18,040 kg into an interplanetary (or NEO intercepting) trajectory. Equation 6.1 implies that an impactor with high density would be most effective in diverting a NEO. Lead has high density and is inexpensive enough to be a reasonable candidate for use as a kinetic impactor. While the impactor would involve both guidance systems and concentrated mass, a fair approximation is to use the density of lead, which is 11 g/cm^3. The closing velocity of the kinetic impactor is a function of the trajectory chosen to achieve intercept. For this analysis, a median closing velocity of 20 km/s was chosen.

A search of unclassified documentation determined that the largest single nuclear warhead yield in a currently deployed strategic system is 24 Mt (Janes, 1996). This is the warhead used in the Russian SS-18 Mod 1 missile, appropriately nicknamed "Satan." Since no information about the warhead mass was available, it was assumed to be less than the 18,040 kg useful payload of the Energia launch vehicle. The neutron production efficiency (n) can vary from 0.03 to 0.3 (Elder, 1997, p. 43). A median value of $n = 0.15$ was chosen for this analysis. The geometrical efficiency factor (A) is taken from a standoff distance of 0.4 NEO radii to give a value of $A = 0.3$ (Ahrens, 1994, p. 912).

Finally, the results assume that the ΔV is applied in an optimal direction.

All assumptions used for analysis of the capability of current mitigation technologies are summarized as follows:

NEO Physical Properties	
Yield strength	$Y = 10^8$ dyne/cm^2
Density	$\rho = 3\times10^3$ kg/m^3
Kinetic Impactor	
Mass	$M_i = 18{,}040$ kg
Density	$\rho_i = 11$ g/cm^3
Closing Velocity	$v_i = 20$ km/s
Nuclear	
Yield	$W = 24$ Mt
Neutron Production	$n = 0.15$
Geometrical Efficiency	$A = 0.3$
Optimal Impulse Direction	
Single Diversion Mission	

Table 6.1 Assumptions Used in Mitigation Capability Analysis

E.   TOUTATIS

The asteroid Toutatis is an Earth-Crossing Asteroid that passes within 10 lunar distances every four years (Park, 1997, p. 9). Its low inclination makes it suitable for analysis with the planar methods used in this thesis. The orbital parameters of Toutatis are as follows:

$a = 2.5154$ AU

$e = 0.6361$

$i = 0.47°$

To apply the analysis to Toutatis, it must be assumed that i=0°. This condition is necessary to create an impact with the Earth, as well as to conform with the assumptions made in the patched conic analysis.

Toutatis takes the shape of two attached spheres which combine to give a diameter of approximately 4.3 km (Elder, 1997, p. 45).

Figure 6.1 indicates the capability of the three impulse technologies against the Toutatis-type asteroid. The Figure shows a plot of the NEO's diameter versus the impulse time in Earth years. It should be noted that the critical properties that define the amount of energy required for mitigation is the minimum ΔV and the NEO mass. The NEO's density was assumed above. This assumption allows calculation of NEO diameter, assuming a spherical NEO. Since the NEO diameter is somewhat easier to identify with than its mass, the diameter is used in these plots.
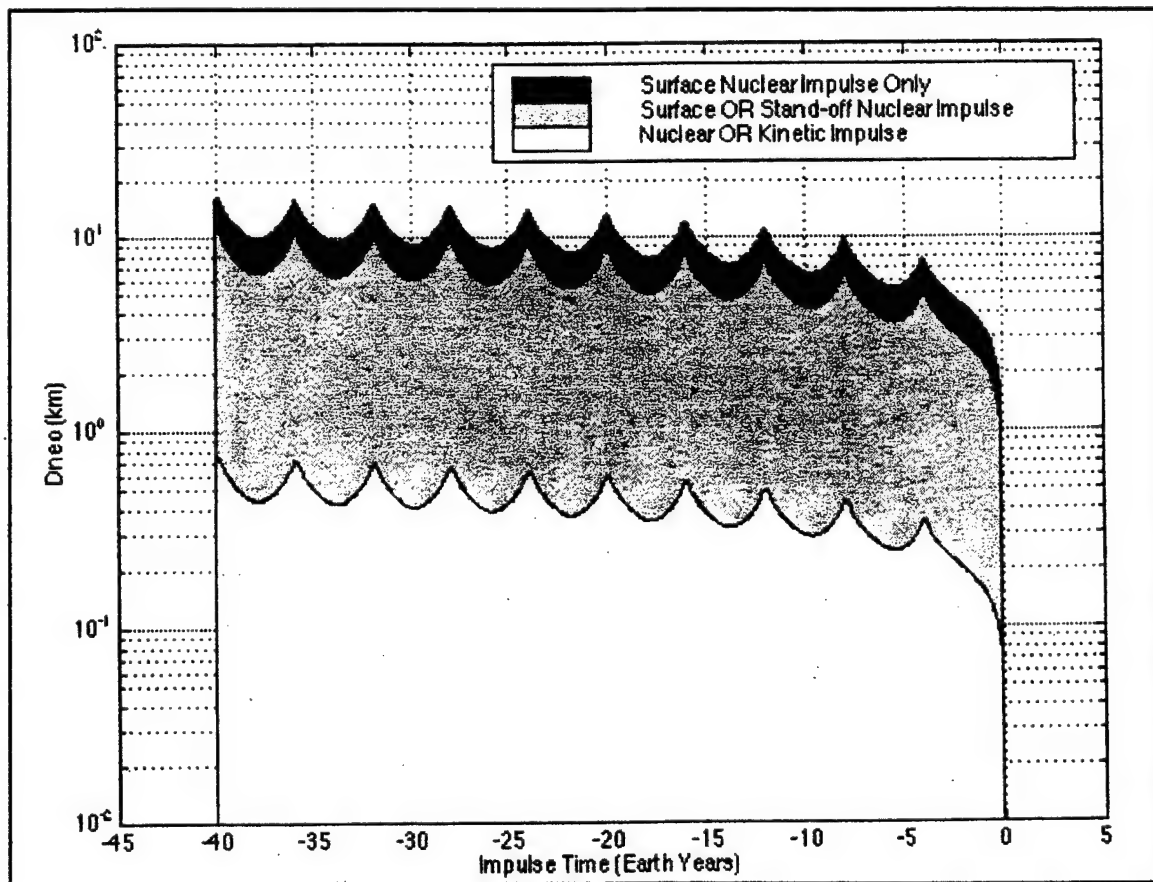
Figure 6.1 Mitigation Capability Against NEOs in Toutatis-type Orbit

It is apparent from Figure 6.1 that Toutatis-type NEOs cannot be deflected with a single kinetic impulse for many years. The diameter of Toutatis (4.3 km) lies comfortably within the capability of either nuclear option. However, Figure 6.2 shows

that a short warning impact from Toutatis cannot be deflected with any single mission. This Figure shows the deflection capability within one period of Toutatis. From this Figure, it is apparent that a surface nuclear impulse can deflect a Toutatis-type asteroid when the impulse is applied as close as 2 Earth years before impact. If the impulse is applied any closer than that, multiple missions will be required.
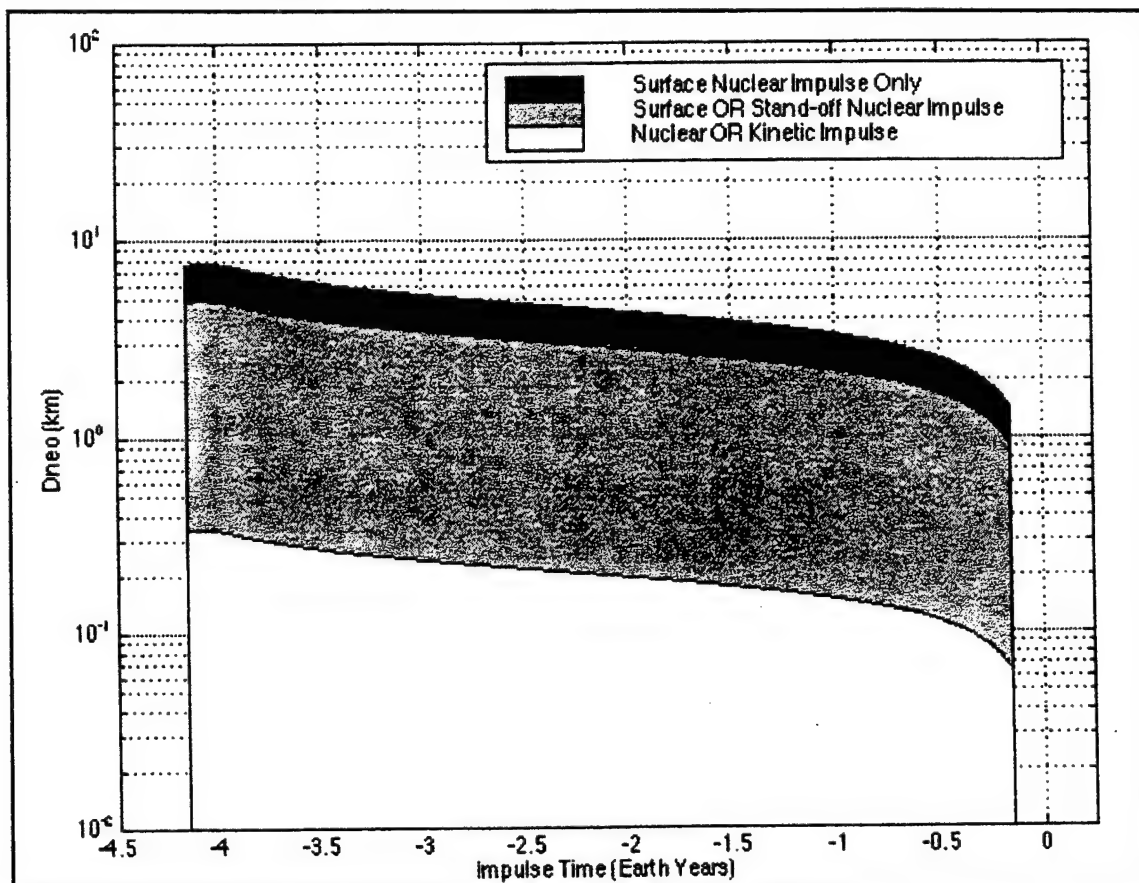
Figure 6.2 Short Warning Mitigation Capability Against NEOs in a Toutatis-like Orbit

F.   NEREUS

For comparison, a second asteroid in a more circular orbit that Toutatis was analyzed. The orbital parameters of the asteroid Nereus meet the criteria, and are listed below (NASA Ames):

$$a = 1.4897 \text{ AU}$$

$$e = 0.3602$$

$$i = 1.41°$$

$$D = 0.8 \text{ km}$$

Although this asteroid is significantly smaller than Toutatis, the long range plot in Figure 6.3 indicates that the kinetic impactor is still insufficient as early as 18 years before impact. However, it can be deflected with a single mission as close as 0.2 Earth years before impact, as indicated in Figure 6.4.
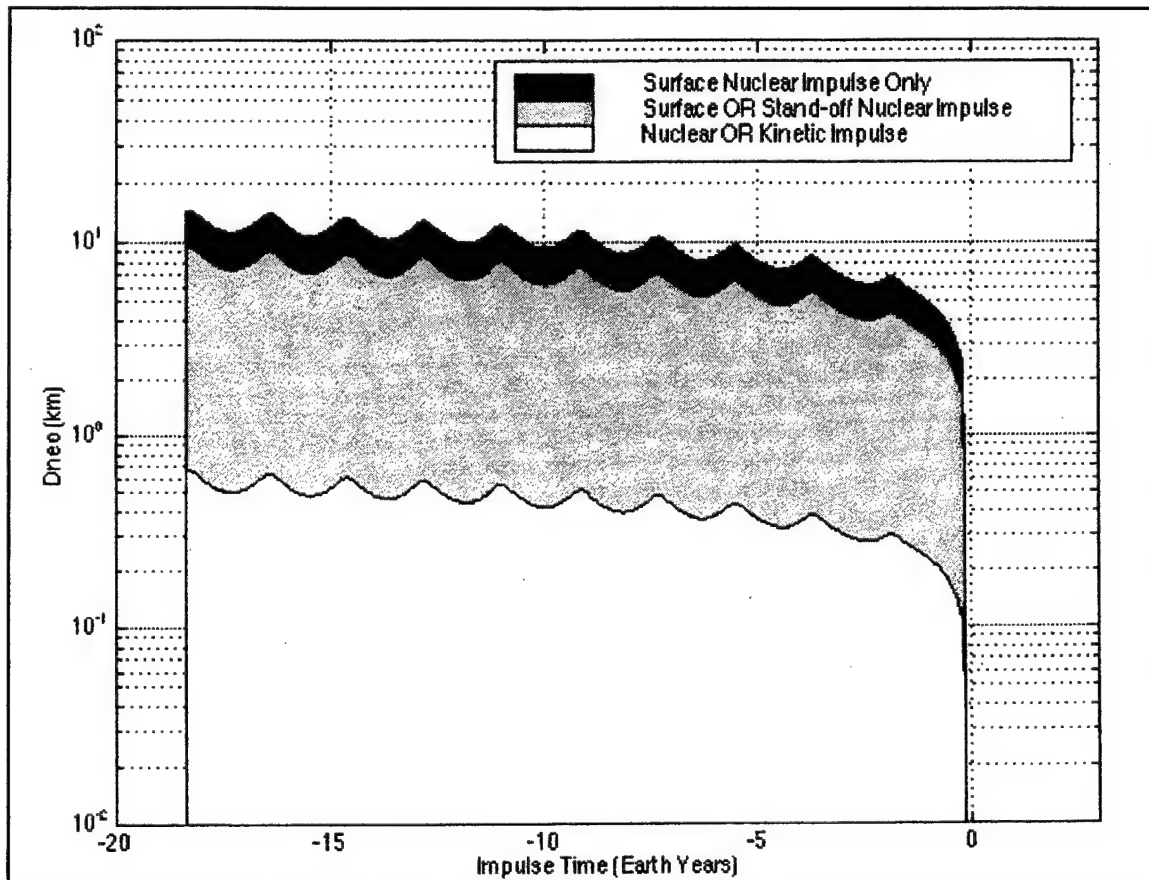
Figure 6.3 Mitigation Capability Against NEOs in Nereus-type Orbits
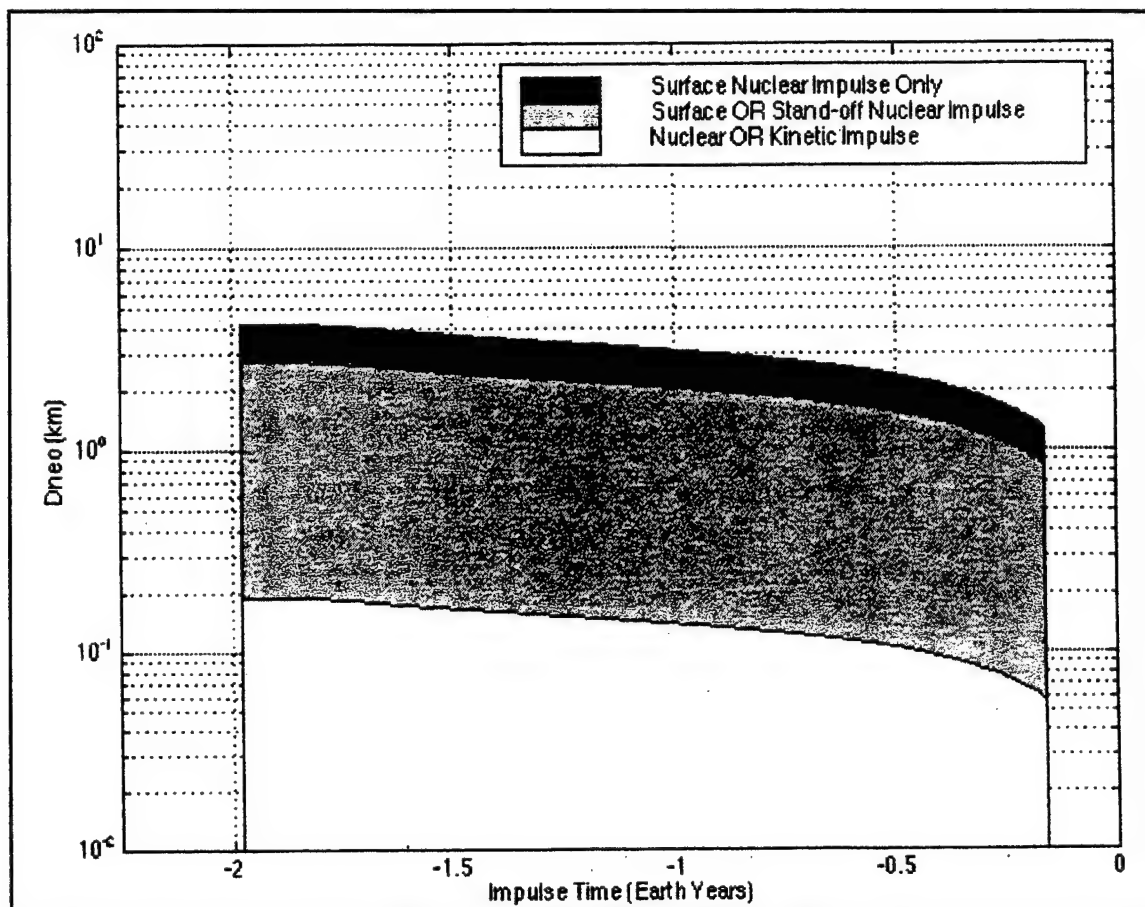
Figure 6.4   Short Warning Mitigation Capability Against NEOs in a Nereus-like Orbit

VII.   SUMMARY AND RECOMMENDATIONS FOR FURTHER WORK

A.   SUMMARY

The gravitational effects of the Earth have the strongest influence on minimum ΔV calculations for deflecting NEOs in nearly circular heliocentric orbits. Incorporating the Earth's gravitational effects can increase the minimum ΔV required for deflection by several times the value calculated using a two-body approximation. By combining a detailed understanding of the ΔV requirements for NEO deflection with the analysis of energy coupling by Ahrens and Harris (Ahrens, 1994, p. 897), an estimate of the capability of current impulsive technologies can be made. It is important to remember that the analysis presented in Chapter VI is not precise. Many approximations and assumptions were combined to provide an educated estimate of a single mission capability. Significant amounts of testing, including an actual NEO deflection, will be required to build upon and confirm this analysis. Also, there were several assumptions made in the patched-conic analysis for simplification. While the results are accurate, and give good insight into the dynamics of a deflection mission, it must be remembered that the numbers are presented for NEOs in elliptical orbits that are co-planar with the Earth's orbit. The need to extend the analysis into the third dimension is discussed as a recommendation for further study.

B.   RECOMMENDATIONS FOR FURTHER STUDY

1.   Three-Body Truth Model

A significant amount of work has now been accomplished towards understanding the orbital mechanics that govern a NEO deflection mission. The best way to test this analysis, barring an actual NEO deflection test mission, would be to build a computer

truth model. This computer code could model the three-body dynamics between the Sun, the NEO, and the Earth. A minimum ΔV from the above analysis can be applied in this model to confirm that the NEO is diverted as intended.

The equations of motion for this code are a modified version of the solution to the classic circular restricted three-body problem. In the classic problem, two massive primaries are established in a circular orbit about their center of mass (Weisel, 1997, p. 278). The third body orbits according to the gravitational influence of the two primaries. In the modified circular restricted three-body problem, one of the primaries (the Sun) is significantly more massive than both of the remaining bodies. As such, the second primary (the Earth) is established in a circular orbit not around the center of mass of the primaries, but the center of mass of the Sun. The geometry is shown in Figure 7.1.
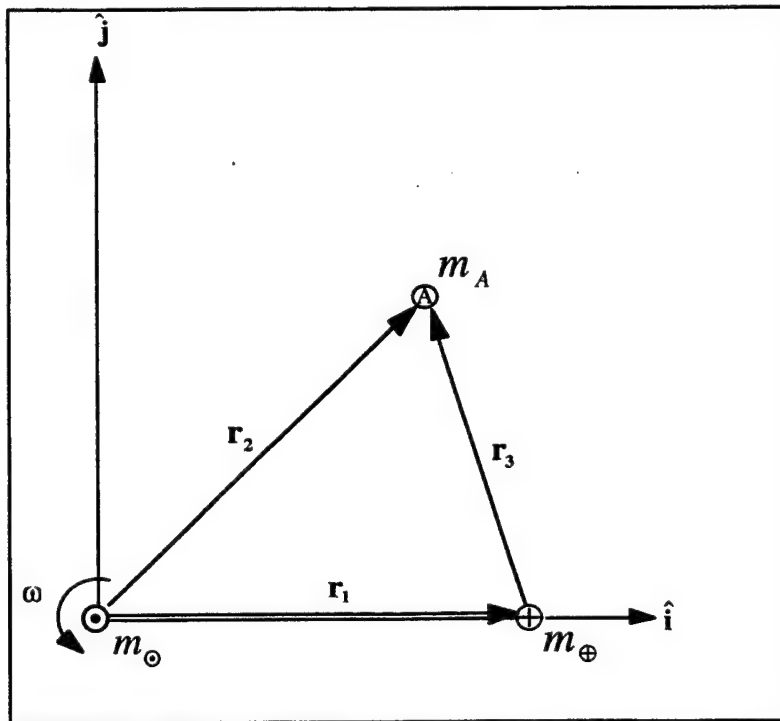
Figure 7.1 Truth Model Geometry

The **ij**-coordinate frame rotates about the Sun's center of mass at a rate ω equal to the rotation rate of the Earth about the Sun. The Earth lies along the **i**-axis at a fixed distance x_1.

62

First, consider the equations of motion as governed by Newton's Laws of Motion and Gravity (Wiesel, 1997, p. 35)

$$m_i \ddot{\mathbf{r}}_i = \sum_{j \neq i}^{N} \frac{Gm_i m_j}{r_{ij}^2} \frac{\mathbf{r}_j - \mathbf{r}_i}{r_{ij}} \tag{7.1}$$

Applying Equation 7.1 to the three body problem shown in Figure 7.1 gives

$$m_A \ddot{\mathbf{r}}_2 = \frac{Gm_\odot m_A}{r_2^3}(0 - \mathbf{r}_2) + \frac{Gm_\oplus m_A}{r_3^3}(\mathbf{r}_1 - \mathbf{r}_2) \tag{7.2}$$

The zero in the first term of Equation 7.2 comes from the fact that the Sun is located at the inertial reference point. Dividing through by m_A and performing some vector algebra gives

$$\ddot{\mathbf{r}}_2 = -\frac{Gm_\odot}{r_2^3} \mathbf{r}_2 - \frac{Gm_\oplus}{r_3^3} \mathbf{r}_3 \tag{7.3}$$

The choice of $\mathbf{r}_2$ rather than $\mathbf{r}_3$ for the equations of motion now becomes apparent. By using $\mathbf{r}_2$, the mass of the NEO cancels out while the mass of the two primaries (the Sun and the Earth) remains. Thus Equation 7.3 explains the gravitational force of the Sun and Earth applied to a NEO per unit mass.

Some manipulation will provide the acceleration in terms of the coordinate system components

$$\ddot{\mathbf{r}}_2 = -\frac{Gm_\odot}{r_2^3}\left(x_2\hat{\mathbf{i}} + y_2\hat{\mathbf{j}}\right) - \frac{Gm_\oplus}{r_3^3}\left(x_3\hat{\mathbf{i}} + y_3\hat{\mathbf{j}}\right) \tag{7.4}$$

$$= -G\left(\frac{m_\odot}{r_2^3}x_2 + \frac{m_\oplus}{r_3^3}x_3\right)\hat{\mathbf{i}} - G\left(\frac{m_\odot}{r_2^3}y_2 + \frac{m_\oplus}{r_3^3}y_3\right)\hat{\mathbf{j}} \tag{7.5}$$

A useful result would be to reduce Equation 7.5 to two variables (x_2 and y_2). This can be accomplished by use of some vector relations.

$$\mathbf{r}_1 + \mathbf{r}_3 = \mathbf{r}_2 \tag{7.6}$$

$$\mathbf{r}_3 = \mathbf{r}_2 - \mathbf{r}_1 \tag{7.7}$$

Thus

63

$$x_3\hat{\mathbf{i}} + y_3\hat{\mathbf{j}} = (x_2 - x_1)\hat{\mathbf{i}} + (y_2 - y_1)\hat{\mathbf{j}} \tag{7.8}$$

In the $\hat{\mathbf{i}}$-component, x_2 is a variable but x_1 is a known fixed distance of 1 AU. The $\hat{\mathbf{j}}$-component reduces to y_2 because y_1 is defined to be equal to zero. Placing these results into Equation 7.5 gives

$$\ddot{\mathbf{r}}_2 = -G\left[\frac{m_\odot}{r_2^3}x_2 + \frac{m_\oplus}{r_3^3}(x_2 - 1AU)\right]\hat{\mathbf{i}} - Gy_2\left[\frac{m_\odot}{r_2^3} + \frac{m_\oplus}{r_3^3}\right]\hat{\mathbf{j}} \tag{7.9}$$

The two radii can be expressed in terms of x_2, y_2, and the known variable x_1 as follows

$$r_2 = \sqrt{x_2^2 + y_2^2} \tag{7.10}$$

$$r_3 = \sqrt{(x_2 - 1AU)^2 + y_2^2} \tag{7.11}$$

Equation 7.9 is the equation of motion of the NEO in the three-body coordinate system. Now it is necessary to investigate the dynamics of the system. Beginning with the definition of the $\mathbf{r}_2$ vector, the velocity can be derived as follows:

$$\mathbf{r}_2 = x_2\hat{\mathbf{i}} + y_2\hat{\mathbf{j}} \tag{7.12}$$

$$\dot{\mathbf{r}}_2 = \dot{x}_2\hat{\mathbf{i}} + x_2\dot{\hat{\mathbf{i}}} + \dot{y}_2\hat{\mathbf{j}} + y_2\dot{\hat{\mathbf{j}}} \tag{7.13}$$

The Transportation Theorem (Greenwood, 1988, p. 49) must be applied because the coordinate system is rotating about the $\hat{\mathbf{k}}$-axis. This Theorem states that

$$\dot{\hat{\mathbf{i}}} = \omega\hat{\mathbf{k}} \times \hat{\mathbf{i}} = \omega\hat{\mathbf{j}} \tag{7.14}$$

and

$$\dot{\hat{\mathbf{j}}} = \omega\hat{\mathbf{k}} \times \hat{\mathbf{j}} = -\omega\hat{\mathbf{i}} \tag{7.15}$$

Substitution of Equations 7.14 and 7.15 into Equation 7.13 yields

$$\dot{\mathbf{r}}_2 = \dot{x}_2\hat{\mathbf{i}} + x_2\left(\omega\hat{\mathbf{j}}\right) + \dot{y}_2\hat{\mathbf{j}} + y_2\left(-\omega\hat{\mathbf{i}}\right) \tag{7.16}$$

$$= (\dot{x}_2 - \omega y_2)\hat{\mathbf{i}} + (\dot{y}_2 + \omega x_2)\hat{\mathbf{j}} \tag{7.17}$$

The velocity can now be differentiated to give the acceleration

$$\ddot{\mathbf{r}}_2 = (\ddot{x}_2 - \omega\dot{y}_2)\hat{\mathbf{i}} + (\dot{x}_2 - \omega y_2)\dot{\hat{\mathbf{i}}} + (\ddot{y}_2 + \omega\dot{x}_2)\hat{\mathbf{j}} + (\dot{y}_2 + \omega x_2)\dot{\hat{\mathbf{j}}} \tag{7.18}$$

$$= (\ddot{x}_2 - \omega\dot{y}_2)\hat{\mathbf{i}} + (\dot{x}_2 - \omega y_2)(\omega\hat{\mathbf{j}}) + (\ddot{y}_2 + \omega\dot{x}_2)\hat{\mathbf{j}} + (\dot{y}_2 + \omega x_2)(-\omega\hat{\mathbf{i}}) \quad (7.19)$$

$$\boxed{\ddot{\mathbf{r}}_2 = (\ddot{x}_2 - 2\omega\dot{y}_2 - \omega^2 x_2)\hat{\mathbf{i}} + (\ddot{y}_2 + 2\omega\dot{x}_2 - \omega^2 y_2)\hat{\mathbf{j}}} \quad (7.20)$$

Equation 7.20 defines the dynamics of the three-body problem in the rotating coordinate system. To convert to a state-space form useful in building the truth model, the components of Equations 7.9 and 7.20 are equated. This process yields the following final relations

$$\boxed{\begin{aligned} \ddot{x}_2 - 2\omega\dot{y}_2 - \omega^2 x_2 &= -G\left[\frac{m_\odot}{r_2^3}x_2 + \frac{m_\oplus}{r_3^3}(x_2 - x_1)\right] \\ \ddot{y}_2 + 2\omega\dot{x}_2 - \omega^2 y_2 &= -G y_2\left(\frac{m_\odot}{r_2^3} + \frac{m_\oplus}{r_3^3}\right) \\ r_2 &= \sqrt{x_2^2 + y_2^2} \\ r_3 &= \sqrt{(x_2 - 1AU)^2 + y_2^2} \end{aligned}} \quad (7.21)$$

With Equations 7.21, the motion of the NEO has been described using two second order differential equations. Because the equations are non-linear, the best solution is to convert to a state-space form and resolve them numerically on a computer. The truth model can then confirm that r_3 equals the desired minimum as calculated in the EDAI code.

2. Three-Dimensional Analysis

The assumption of co-planar orbits greatly simplified the above analysis, but it also severely limited the practicable application of the analysis. Generalizing the theory to three dimensions is critical in application to the majority of hazardous NEOs.

3. Hyperbolic Orbital Analysis

There are two points where a detailed hyperbolic analysis can be added to the NEO mitigation analysis. First, many NEOs can be established in a hyperbolic orbit

about the Sun before impact with the Earth. These orbits were not included in this thesis. Second, the effectiveness of an impulse applied within the sphere of influence of the Earth was not investigated in this thesis. Both areas are important for a thorough understanding of the NEO impact problem.

4.   EDAI Code Development

The EDAI code has great potential to be very useful in designing a mitigation plan. As currently written, the code generates a minimum ΔV required to generate a given miss distance. By adding the analysis included in Chapter VI, the code could produce a more useful result, namely the ability of a proposed mission to effectively mitigate a known threat. In a fully developed code, the user should be able to input NEO's orbital parameters (including the inclination with respect to the ecliptic), the NEO's physical properties, and the properties of proposed mitigation efforts. The code would then output a plot of the mitigation capability against the diameter or mass of the threat-NEO, as in Figure 6.1. The user could then determine if the mitigation effort is sufficient to handle potential errors in estimates of the NEO's physical properties.

As the first user not involved in the writing of the code, it would be constructive to provide suggestions for improvement. With some improvements and further testing, the code could be widely used in researching the hazard mitigation problem.

The importance of an accurate initial guess was discussed in Chapter V. As currently written, a user is required to directly modify the code to input a new initial guess. A possible improvement would be to allow the user to input an initial guess. However, this would require a fairly well-educated guess, which is difficult to make without a thorough understanding of the problem. Another option for improvement would be to build a reference file of results from previous successful runs. This reference file could be accessed once the user has input the orbital parameters of interest to get an accurate initial guess.

66

Chapter V also discusses an instability induced by round-off error. The solution to this problem is to run the code with a larger minimum separation (e.g., 10 $R_\oplus$) and divide the result to achieve the desired separation (e.g., divide by 10). A more robust code could test for potential round-off instabilities and eliminate this complication for the user.

It would be helpful to have the ability to name the output file during initialization while the code is actually running. This would eliminate the need to alter the code to rename the output file. Also, adding the NEO's orbital parameters and the required separation distance to the output file could help to avoid confusion between different files.

A minor bug in the code was discovered when analyzing NEO orbits with a semi-major axis equal to 1 AU. In this unique case, the period of the NEO is identical to the period of the Earth. Thus, an impact would occur after each NEO period. The EDAI code, however, only calculates the minimum ΔV required to divert the NEO for a specific impact time. The code does not recognize that impact will occur after each orbital period. Thus, the results indicate that a ΔV applied several periods before impact will have a greater effect than a ΔV applied within an orbital period of impact. In reality, the results should be the same for each period.

5.   Billiards Scenario

There is a fourth potential impulse concept that was not investigated in this analysis. Melosh , Nemchinov, and Zetzer (Melosh, 1994, p. 1115) suggest diverting a smaller NEO into a large threatening NEO. It could be useful to investigate this proposal using techniques developed in this thesis.

6.   Verify Results

The hypothesis discussed in Chapter V that the three-body results differ from the two-body results by a factor exactly equal to the impact radius needs to be verified.

APPENDIX A. V∞ PLOT M-FILE

```
%   Vasterth3.m

%   This m-file plots the magnitude of the velocity of an asteroid, relative
%   to the Earth, at the impact point.   The variables are a_ast_sun and e_ast_sun.
%   Assumptions are:
%
%   -   The Earth is in a circular orbit

clear

%   First set some constants
mu_sun = 1.32712438e11;              %   km^3/s^2
mu_erth = 3.986005e5;               %   km^3/s^2
r_erth_sun = 1.4959787e8;           %   km
R_sun = 6.96e5;                     %   km
a_min = (r_erth_sun + R_sun)/2;     %   km
a_max = 10*r_erth_sun;              %   km
Re = 6378;                          %   km
n_max = 50;

%   The first FOR-loop varies e from 0 to 1 at a step of 0.1
for n = 1:(n_max - 1)

%   The next (imbedded) FOR-loop varies a from a_min to a_max
    for step = 1:(n_max - 1)
        e(n,step) = n/n_max;
        a(n,step) = (step - 1)*(a_max - a_min)/50 + a_min;

%   Check that the orbital parameters define an orbit that intersects the Earth's
%     orbit.
        if a(n,step)*(1-e(n,step)) > r_erth_sun

            V_ast_erth(n,step) = 0;
            bi(n,step) = 0;

        elseif a(n,step)*(1+e(n,step)) < r_erth_sun

            V_ast_erth(n,step) = 0;
            bi(n,step) = 0;

        else

%   If the asteroid's orbit will intersect the Earth's orbit, compute the true anomaly
%     of the impact and the flight path angle at impact.
            nu_imp_erth(n,step) = acos((a(n,step)*(1-e(n,step)^2))/(e(n,step)*r_erth_sun) - 1/
e(n,step));
            gamma_imp(n,step) = atan((e(n,step)*sin(nu_imp_erth(n,step)))/(1 + e(n,step)*
cos(nu_imp_erth(n,step))));
```

```
%   Then compute the magnitude of the velocity of the asteroid with respect to Earth.
        Vx1_ast_erth(n,step) = sqrt((2*mu_sun)/r_erth_sun - mu_sun/a(n,step))*
cos(gamma_imp(n,step));
        Vx_ast_erth(n,step) = Vx1_ast_erth(n,step) - sqrt(mu_sun/r_erth_sun);
        Vy_ast_erth(n,step) = sqrt((2*mu_sun)/r_erth_sun - mu_sun/a(n,step))*
sin(gamma_imp(n,step));
        V_ast_erth(n,step) = sqrt(Vx_ast_erth(n,step)^2 + Vy_ast_erth(n,step)^2);
        bi(n,step) = sqrt((2*mu_erth)/(Re*V_ast_erth(n,step)^2) + 1);        % Re
        end

    [Vmax(n),i] = max(V_ast_erth(n,:));
    aVmax(n) = a(n,i)/r_erth_sun;
    eVmax(n) = n/n_max;
    [bimax(n),j] = max(bi(n,:));
    abimax(n) = a(n,j)/r_erth_sun;
    ebimax(n) = n/n_max;
    end
end

figure(1)
    colormap('white')
    aplot = a/r_erth_sun;
    surf(aplot,e,V_ast_erth)
    grid on
    xlabel('a (AU)')
    ylabel('e')
    zlabel('V_i_n_f_i_n_i_t_y (km/s)')
    title('V_i_n_f_i_n_i_t_y vs. a,e')

figure(2)
    colormap('white')
    surfl(aplot,e,bi)
    grid on
    xlabel('a (AU)')
    ylabel('e')
    zlabel('b_i (Re)')
    title('Impact Radius (b_i) vs. a,e')
    view(-37.5-125, 30)

answer = input('Generate 2-D impact radius plot? (y/n) ','s');
while answer=='y';
    e_interest = input('At which eccentricity? ');
    index = round(e_interest*n_max);
    figure(3)
    plot(aplot(index,:),bi(index,:))
    grid on
    xlabel ('a (AU)')
    ylabel ('bi (Re)')
    e_title=num2str(e_interest);
    title(['bi vs. a for e = ',e_title])
    print_ans = input('Print 2-D plot? (y/n) ','s');
    if print_ans == 'y'
        figure(3)
        print
    end
    answer = input('Generate 2-D impact radius plot? (y/n) ','s');
end
```

File name: vbnd9.mws
Last Modified: 5 August 1997

Written by: LT Scott Porter

Purpose: 1. Determine if the impact velocity between the Earth and an asteroid in an elliptical orbit has a maximum.

2. If a maximum exists, find a function of an asteoid's semi-major axis and it's eccentricity which results in the maximum impact velocity between the Earth and an asteroid.

This analysis uses the prinicples of orbital mechanics, vector algebra, and simple calculus to determine if the relative velocity between an asteroid and the Earth at impact has a maximum. The asteroid is assumed to be in an elliptical orbit which is co-planar with the Earth's orbit. The Earth is assumed to be in a circular orbit.

```
> restart: with(linalg): readlib(isolate):
```
Warning, new definition for norm
Warning, new definition for trace
Express the magnitude of the velocity of the Earth and the asteroid.

```
> v[E](a):=sqrt(mu[sun]/r[E,sun]);
> v[A,sun](a):=sqrt(2*mu[sun]/r[E,sun] - mu[sun]/a);
```

$$v_E(a) := \sqrt{\frac{\mu_{sun}}{r_{E,sun}}}$$

$$v_{A,sun}(a) := \sqrt{2\frac{\mu_{sun}}{r_{E,sun}} - \frac{\mu_{sun}}{a}}$$

Convert these velocities to vector form. The coordinate system is defined with the X-Y plane in the orbital plane, the origin at the center of mass of the Earth, and the Y-axis continuosly pointing to the center of mass of the Sun. Thus, the velocity of the Earth is always fixed along the X-axis. The velocity of the asteroid is defined by the flight path angle (Gamma(a)), the angle between a tangent to a circle at the asteroid's radius and the velocity vector.

```
> V[E,sun](a):=vector(2,[v[E](a),0]);
> V[A,sun](a):=vector(2,[v[A,sun](a)*cos(Gamma(a)),v[A,sun](a)*sin(G
  amma(a))]);
```

$$V_{E.sun}(a) := \left[\sqrt{\frac{\mu_{sun}}{r_{E.sun}}}, 0 \right]$$

$$V_{A.sun}(a) := \left[\sqrt{2\frac{\mu_{sun}}{r_{E.sun}} - \frac{\mu_{sun}}{a}} \cos(\Gamma(a)), \sqrt{2\frac{\mu_{sun}}{r_{E.sun}} - \frac{\mu_{sun}}{a}} \sin(\Gamma(a)) \right]$$

Using vector algebra, define the velocity of the asteroid with respect to the Earth (V[A,E]). V[A,E] is defined as the velocity of the asteroid with respect to the sun (V[A,sun]) minus the velocity of the Earth with respect to the sun (V[E,sun]).

```
> V[A,E](a):=evalm(V[A,sun](a)-V[E,sun](a));
```

$$V_{A.E}(a) := \left[\sqrt{2\frac{\mu_{sun}}{r_{E.sun}} - \frac{\mu_{sun}}{a}} \cos(\Gamma(a)) - \sqrt{\frac{\mu_{sun}}{r_{E.sun}}}, \sqrt{2\frac{\mu_{sun}}{r_{E.sun}} - \frac{\mu_{sun}}{a}} \sin(\Gamma(a)) \right]$$

Now determine the orbital position and flight path angle of the asteroid at Earth impact.

```
> nu[I](a):=arccos((a*(1-e^2)/(e*r[E,sun])) - 1/e);
> Gamma1(a):=arctan(e*sin(nu[I](a))/(1+e*cos(nu[I](a))));
```

$$v_I(a) := \pi - \arccos\left(-\frac{a(1-e^2)}{e\, r_{E.sun}} + \frac{1}{e} \right)$$

$$\Gamma1(a) := \arctan\left(\frac{e\sqrt{1 - \left(-\frac{a(1-e^2)}{e\, r_{E.sun}} + \frac{1}{e} \right)^2}}{1 + e\left(\frac{a(1-e^2)}{e\, r_{E.sun}} - \frac{1}{e} \right)} \right)$$

```
> Gamma1(a):=simplify(");
```

$$\Gamma1(a) := -\arctan\left(\frac{e\sqrt{-\frac{(-1+e^2)(a^2 e^2 - r_{E.sun}^2 + 2\, a\, r_{E.sun} - a^2)}{e^2\, r_{E.sun}^2}}\, r_{E.sun}}{a(-1+e^2)} \right)$$

Substitute the impact orbital parameters to determine the velocity of the asteroid with respect to the Earth at impact.

```
> V[A,E](a):=subs(Gamma(a)=Gamma1(a),V[A,E](a));
```

$$V_{A.E}(a) := \left[\vphantom{\rule{0pt}{3cm}} \right.$$

$$\sqrt{2\frac{\mu_{sun}}{r_{E.sun}}-\frac{\mu_{sun}}{a}}\cos\left(-\arctan\left(\frac{e\sqrt{-\dfrac{(-1+e^2)(a^2e^2-r_{E.sun}^2+2ar_{E.sun}-a^2)}{e^2r_{E.sun}^2}}\,r_{E.sun}}{a(-1+e^2)}\right)\right)$$

$$-\sqrt{\frac{\mu_{sun}}{r_{E.sun}}},$$

$$\sqrt{2\frac{\mu_{sun}}{r_{E.sun}}-\frac{\mu_{sun}}{a}}\sin\left(-\arctan\left(\frac{e\sqrt{-\dfrac{(-1+e^2)(a^2e^2-r_{E.sun}^2+2ar_{E.sun}-a^2)}{e^2r_{E.sun}^2}}\,r_{E.sun}}{a(-1+e^2)}\right)\right)\Bigg]$$

Now go through several steps to simplify the expression.

```
> V[A,E](a):=vector(2,[simplify(V[A,E](a)[1]),simplify(V[A,E](a)[2])
  ]);
```

$$V_{A.E}(a):=\left[\frac{\sqrt{\dfrac{\mu_{sun}(-r_{E.sun}+2a)}{ar_{E.sun}}}-\sqrt{\dfrac{\mu_{sun}}{r_{E.sun}}}\sqrt{-\dfrac{r_{E.sun}(-r_{E.sun}+2a)}{(-1+e^2)a^2}}}{\sqrt{-\dfrac{r_{E.sun}(-r_{E.sun}+2a)}{(-1+e^2)a^2}}},\right.$$

$$\left.-\frac{\sqrt{\dfrac{\mu_{sun}(-r_{E.sun}+2a)}{ar_{E.sun}}}\,e\sqrt{-\dfrac{(-1+e^2)(a^2e^2-r_{E.sun}^2+2ar_{E.sun}-a^2)}{e^2r_{E.sun}^2}}\,r_{E.sun}}{a(-1+e^2)\sqrt{-\dfrac{r_{E.sun}(-r_{E.sun}+2a)}{(-1+e^2)a^2}}}\right]$$

```
> V2[A,E](a):=vector(2,[combine(V[A,E](a)[1]),combine(V[A,E](a)[2])]
  );
```

$$V2_{A.E}(a):=\left[\frac{\sqrt{\dfrac{\mu_{sun}(-r_{E.sun}+2a)}{ar_{E.sun}}}-\dfrac{\sqrt{(\mu_{sun}r_{E.sun}-2\mu_{sun}a)(-a^2+a^2e^2)}}{-a^2+a^2e^2}}{\sqrt{-\dfrac{r_{E.sun}(-r_{E.sun}+2a)}{(-1+e^2)a^2}}},\,((\right.$$

$$\mu_{sun}a^2e^2r_{E.sun}^2-4\mu_{sun}a^3e^2r_{E.sun}+4\mu_{sun}a^4e^2-\mu_{sun}r_{E.sun}^4+6\mu_{sun}r_{E.sun}^3a-13\mu_{sun}r_{E.sun}^2a^2$$

$$+ 12\,\mu_{sun}\,a^3\,r_{E.\,sun} - 4\,\mu_{sun}\,a^4)\,a)^{1/2} \Big/ (a\,(-r_{E.\,sun} + 2\,a)\,r_{E.\,sun})$$

```
> V3[A,E] (a) :=vector(2,[expand(V2[A,E] (a) [1]),expand(V2[A,E] (a) [2])]
 );
```

$$V3_{A.\,E}(a) :=$$

$$\frac{\sqrt{2\,\dfrac{\mu_{sun}}{r_{E.\,sun}} - \dfrac{\mu_{sun}}{a}}}{\sqrt{\dfrac{r_{E.\,sun}^{2}}{(-1+e^2)\,a^2} - 2\,\dfrac{r_{E.\,sun}}{(-1+e^2)\,a}}} - \frac{\sqrt{-\mu_{sun}\,r_{E.\,sun}\,a^2 + \mu_{sun}\,r_{E.\,sun}\,a^2\,e^2 + 2\,\mu_{sun}\,a^3 - 2\,\mu_{sun}\,a^3\,e^2}}{\sqrt{\dfrac{r_{E.\,sun}^{2}}{(-1+e^2)\,a^2} - 2\,\dfrac{r_{E.\,sun}}{(-1+e^2)\,a}}\,(-a^2 + a^2\,e^2)},$$

$$(\mu_{sun}\,a^3\,e^2\,r_{E.\,sun}^{2} - 4\,\mu_{sun}\,a^4\,e^2\,r_{E.\,sun} + 4\,\mu_{sun}\,a^5\,e^2 - a\,\mu_{sun}\,r_{E.\,sun}^{4} + 6\,\mu_{sun}\,r_{E.\,sun}^{3}\,a^2$$

$$- 13\,\mu_{sun}\,r_{E.\,sun}^{2}\,a^3 + 12\,\mu_{sun}\,a^4\,r_{E.\,sun} - 4\,\mu_{sun}\,a^5)^{1/2} \Big/ (a\,(-r_{E.\,sun} + 2\,a)\,r_{E.\,sun})$$

```
> V4[A,E] (a) :=vector(2,[simplify(V3[A,E] (a) [1]),simplify(V3[A,E] (a) [
 2])]);
```

$$V4_{A.\,E}(a) := \left[\left(-\sqrt{\frac{\mu_{sun}\,(-r_{E.\,sun} + 2\,a)}{a\,r_{E.\,sun}}}\,a^2 + \sqrt{\frac{\mu_{sun}\,(-r_{E.\,sun} + 2\,a)}{a\,r_{E.\,sun}}}\,a^2\,e^2\right.\right.$$

$$\left.-\sqrt{-\mu_{sun}\,(-1+e^2)\,a^2\,(-r_{E.\,sun} + 2\,a)}\right) \Big/ \left(\sqrt{-\frac{r_{E.\,sun}\,(-r_{E.\,sun} + 2\,a)}{(-1+e^2)\,a^2}}\,(-1+e^2)\,a^2\right),$$

$$\left.\frac{\sqrt{\mu_{sun}\,(a^2\,e^2 - r_{E.\,sun}^{2} + 2\,a\,r_{E.\,sun} - a^2)\,a\,(-r_{E.\,sun} + 2\,a)^2}}{a\,(-r_{E.\,sun} + 2\,a)\,r_{E.\,sun}}\right]$$

Find the square of the magnitude of the velocity. Using the square of the magnitude, rather than just the magnitude, simplifies the algebra but gives the same final result. The maximum of a function occurs at the same place as the maximum of it's square.

```
> Vmag2[A,E](a):=(V3[A,E](a)[1])^2 + V3[A,E](a)[2]^2;
```

$$Vmag2_{A,E}(a) := \left(\frac{\sqrt{2\frac{\mu_{sun}}{r_{E.sun}} - \frac{\mu_{sun}}{a}}}{\sqrt{\frac{r_{E.sun}^2}{(-1+e^2)a^2} - 2\frac{r_{E.sun}}{(-1+e^2)a}}} - \frac{\sqrt{-\mu_{sun}\,r_{E.sun}\,a^2 + \mu_{sun}\,r_{E.sun}\,a^2\,e^2 + 2\,\mu_{sun}\,a^3 - 2\,\mu_{sun}\,a^3\,e^2}}{\sqrt{\frac{r_{E.sun}^2}{(-1+e^2)a^2} - 2\frac{r_{E.sun}}{(-1+e^2)a}}\,(-a^2 + a^2\,e^2)} \right)^\wedge$$

$$+ \left(\mu_{sun}\,a^3\,e^2\,r_{E.sun}^2 - 4\,\mu_{sun}\,a^4\,e^2\,r_{E.sun} + 4\,\mu_{sun}\,a^5\,e^2 - a\,\mu_{sun}\,r_{E.sun}^4 + 6\,\mu_{sun}\,r_{E.sun}^3\,a^2 \right.$$

$$\left. - 13\,\mu_{sun}\,r_{E.sun}^2\,a^3 + 12\,\mu_{sun}\,a^4\,r_{E.sun} - 4\,\mu_{sun}\,a^5 \right) \Big/ \left(a^2\,(-r_{E.sun} + 2a)^2\,r_{E.sun}^2 \right)$$

Simplify the expression.

```
> Vmag[A,E](a):=simplify(");
```

$$Vmag_{A,E}(a) := \left(-5\,r_{E.sun}\,\mu_{sun}\,a + 6\,\mu_{sun}\,a^2 + \mu_{sun}\,r_{E.sun}^2 \right.$$

$$\left. + 2\,\sqrt{\frac{\mu_{sun}\,(-r_{E.sun} + 2a)}{a\,r_{E.sun}}}\,a\,\sqrt{-\mu_{sun}\,(-1+e^2)\,a^2\,(-r_{E.sun} + 2a)} \right) \Big/ \left(r_{E.sun}\,a\,(-r_{E.sun} + 2a) \right)$$

```
> combine(");
```

$$\left(-5\,r_{E.sun}\,\mu_{sun}\,a + 6\,\mu_{sun}\,a^2 + \mu_{sun}\,r_{E.sun}^2 + 2\,a\,\left(\right. \right.$$

$$\left. \left(\mu_{sun}^2\,a\,r_{E.sun}^2 - 4\,\mu_{sun}^2\,a^2\,r_{E.sun} + 4\,\mu_{sun}^2\,a^3 - \mu_{sun}^2\,a\,e^2\,r_{E.sun}^2 + 4\,\mu_{sun}^2\,a^2\,e^2\,r_{E.sun} - 4\,\mu_{sun}^2\,a^3\,e^2 \right) \right.$$

$$\left. r_{E.sun} \right)^{1/2} \Big/ r_{E.sun} \right) \Big/ \left(r_{E.sun}\,a\,(-r_{E.sun} + 2a) \right)$$

```
> factor(");
```

$$\left(-5\,r_{E.sun}^2\,\mu_{sun}\,a + 6\,\mu_{sun}\,r_{E.sun}\,a^2 + \mu_{sun}\,r_{E.sun}^3 \right.$$

$$\left. + 2\,a\,\sqrt{-\mu_{sun}^2\,a\,(e-1)(e+1)(-r_{E.sun} + 2a)^2\,r_{E.sun}} \right) \Big/ \left(r_{E.sun}^2\,a\,(-r_{E.sun} + 2a) \right)$$

```
> collect(",a);
```

$$\left(6\,\mu_{sun}\,r_{E.sun}\,a^2 + \left(-5\,\mu_{sun}\,r_{E.sun}^2 + 2\,\sqrt{-\mu_{sun}^2\,a\,(e-1)(e+1)(-r_{E.sun} + 2a)^2\,r_{E.sun}} \right) a \right.$$

$$\left. + \mu_{sun}\,r_{E.sun}^3 \right) \Big/ \left(r_{E.sun}^2\,a\,(-r_{E.sun} + 2a) \right)$$

75

```
> Vmagsqrd[A,E](a):=sort(");
```

$$Vmagsqrd_{A,E}(a) := (6 a^2 \mu_{sun} r_{E.sun} + \mu_{sun} r_{E.sun}{}^3$$
$$+ (-5 \mu_{sun} r_{E.sun}{}^2 + 2 \sqrt{-(e-1)(e+1)(2a-r_{E.sun})^2 a \mu_{sun}{}^2 r_{E.sun}}) a) \Big/ ((2a-r_{E.sun}) a$$
$$r_{E.sun}{}^2)$$

Differentiate the function for the magnitude (squared) and set the result equal to zero to find the maximum.

```
> Vmax1[A,E](a):=simplify(diff(Vmagsqrd[A,E](a),a)=0);
```

$$Vmax1_{A,E}(a) := - (-2 \mu_{sun} a^3 + 2 \mu_{sun} a^3 e^2 + a^2 \mu_{sun} r_{E.sun} - \mu_{sun} r_{E.sun} a^2 e^2$$
$$- r_{E.sun} \sqrt{-(e-1)(e+1)(2a-r_{E.sun})^2 a \mu_{sun}{}^2 r_{E.sun}}) \mu_{sun} \Big/ (r_{E.sun} a^2$$
$$\sqrt{-(e-1)(e+1)(2a-r_{E.sun})^2 a \mu_{sun}{}^2 r_{E.sun}}) = 0$$

```
> Vtest[A,E](a):=simplify(diff(Vmax1[A,E](a),a));
```

$$Vtest_{A,E}(a) := \frac{1}{2} (-2 \mu_{sun} a^3 + 2 \mu_{sun} a^3 e^2 + a^2 \mu_{sun} r_{E.sun} - \mu_{sun} r_{E.sun} a^2 e^2$$
$$- 4 r_{E.sun} \sqrt{-(e-1)(e+1)(2a-r_{E.sun})^2 a \mu_{sun}{}^2 r_{E.sun}}) \mu_{sun} \Big/ (a^3$$
$$\sqrt{-(e-1)(e+1)(2a-r_{E.sun})^2 a \mu_{sun}{}^2 r_{E.sun}} r_{E.sun}) = 0$$

Solve this function for the semi-major axis. This result will determine, for a given eccentricity (e), the semi-major axis which will generate the maximum relative velocity between the asteroid and the Earth at impact.

```
> isolate(Vmax1[A,E](a),a);
```

$$a = \frac{(-(-1+e^2))^{2}{}^{1/3} r_{E.sun}}{-1+e^2}$$

```
> subs(a=amax,");
```

$$amax = \frac{(-(-1+e^2))^{2}{}^{1/3} r_{E.sun}}{-1+e^2}$$

```
> assign(");
```

To further simplify the relation, use r[E,sun]=1 AU.

```
> aAU:=subs(r[E,sun]=1,amax);
```

$$aAU := \frac{\left(-\left(-1+e^2\right)^2\right)^{1/3}}{-1+e^2}$$

```
> Vtest2[A,E](a):=subs(a=aAU,Vtest[A,E](a));
```

$$Vtest2_{A,E}(a) := -\frac{1}{2}\left(2\,\frac{\mu_{sun}}{-1+e^2} - 2\,\frac{\mu_{sun}\,e^2}{-1+e^2} + \frac{\left(-\left(-1+e^2\right)^2\right)^{2/3}\mu_{sun}\,r_{E.\,sun}}{\left(-1+e^2\right)^2} \right.$$

$$-\frac{\mu_{sun}\,r_{E.\,sun}\left(-\left(-1+e^2\right)^2\right)^{2/3}e^2}{\left(-1+e^2\right)^2}$$

$$\left. -4\,r_{E.\,sun}\sqrt{-\frac{(e-1)(e+1)\left(2\,\frac{\left(-\left(-1+e^2\right)^2\right)^{1/3}}{-1+e^2} - r_{E.\,sun}\right)^2\left(-\left(-1+e^2\right)^2\right)^{1/3}\mu_{sun}^{\,2}\,r_{E.\,sun}}{-1+e^2}} \right)$$

$$(-1+e^2)\,\mu_{sun} \Bigg/ \sqrt{-\frac{(e-1)(e+1)\left(2\,\frac{\left(-\left(-1+e^2\right)^2\right)^{1/3}}{-1+e^2} - r_{E.\,sun}\right)^2\left(-\left(-1+e^2\right)^2\right)^{1/3}\mu_{sun}^{\,2}\,r_{E.\,sun}}{-1+e^2}}\,r_{E.\,sun} = 0$$

```
> simplify(");
```

$$\frac{1}{2}\frac{\mu_{sun}\left(4\,r_{E.\,sun}\sqrt{\%1}\,e^2 + 2\,\mu_{sun}\,e^2 - 2\,\mu_{sun} - 4\,r_{E.\,sun}\sqrt{\%1} + \left(-\left(-1+e^2\right)^2\right)^{2/3}\mu_{sun}\,r_{E.\,sun}\right)}{r_{E.\,sun}\sqrt{\%1}} = 0$$

$$\%1 := -\frac{\left(-2\left(-\left(-1+e^2\right)^2\right)^{1/3} - r_{E.\,sun} + r_{E.\,sun}\,e^2\right)^2\left(-\left(-1+e^2\right)^2\right)^{1/3}\mu_{sun}^{\,2}\,r_{E.\,sun}}{\left(-1+e^2\right)^2}$$

```
> subs(r[E,sun]=1,");
```

$$\frac{1}{2}\frac{\mu_{sun}\left(4\sqrt{\%1}\,e^2 + 2\,\mu_{sun}\,e^2 - 2\,\mu_{sun} - 4\sqrt{\%1} + \left(-\left(-1+e^2\right)^2\right)^{2/3}\mu_{sun}\right)}{\sqrt{\%1}} = 0$$

$$\%1 := -\frac{\left(-2\left(-\left(-1+e^2\right)^2\right)^{1/3} - 1 + e^2\right)^2\left(-\left(-1+e^2\right)^2\right)^{1/3}\mu_{sun}^{\,2}}{\left(-1+e^2\right)^2}$$

```
> simplify(");
```

$$\frac{1}{2}\frac{\mu_{sun}\,(4\,\sqrt{\%1}\;e^2+2\,\mu_{sun}\,e^2-2\,\mu_{sun}-4\,\sqrt{\%1}\;+(-(-1+e^2)^2)^{2/3}\,\mu_{sun})}{\sqrt{\%1}}=0$$

$$\%1:=-\frac{(-2\,(-(-1+e^2)^2)^{1/3}-1+e^2)^2\,(-(-1+e^2)^2)^{1/3}\,{\mu_{sun}}^2}{(-1+e^2)^2}$$

```
> eval(subs(mu[sun]=1,"));
```

$$\frac{1}{2}\frac{4\,\sqrt{\%1}\;e^2+2\,e^2-2-4\,\sqrt{\%1}\;+(-(-1+e^2)^2)^{2/3}}{\sqrt{\%1}}=0$$

$$\%1:=-\frac{(-2\,(-(-1+e^2)^2)^{1/3}-1+e^2)^2\,(-(-1+e^2)^2)^{1/3}}{(-1+e^2)^2}$$

```
> simplify(");
```

$$\frac{1}{2}\frac{4\,\sqrt{\%1}\;e^2+2\,e^2-2-4\,\sqrt{\%1}\;+(-(-1+e^2)^2)^{2/3}}{\sqrt{\%1}}=0$$

$$\%1:=-\frac{(-2\,(-(-1+e^2)^2)^{1/3}-1+e^2)^2\,(-(-1+e^2)^2)^{1/3}}{(-1+e^2)^2}$$

End of analysis.

78

APPENDIX C. INITIAL GUESSES FOR EDAI CODE

As with any numerical optimization algorithm, the EDAI code requires an accurate initial guess of the results. An inaccurate guess will result in an instability. For this analysis, the code was first run with a known solution used to provide an initial guess. Then the NEO's orbital parameters were altered slightly, such that the initial guess from the previous run was still close enough to the correct answer to provide a stable run. This process was continued until a database of initial guesses was built. The initial guesses are provided here.

Canonical units are used for the ΔV and t_f guesses. The units are defined as follows:

$$DU = \text{Distance Unit} = \text{Astronomical Unit (AU)} = 1.495978e8 \text{ km}$$

$$TU = \text{Time Unit} = \frac{1}{2\pi} \text{ year}$$

e	a (AU)	Minimum Separation ($R_\oplus$)	$\Delta V_\parallel$ (DU/TU)	$\Delta V_\perp$ (DU/TU)	t_f (TU)
0.1	1.0	10	1.062e-7	4.142e-4	2.843e-4
0.2	1.0	10	4.963e-5	4.157e-4	1.336e-4
0.3	1.0	10	-1.581e-5	3.999e-4	8.856e-5
0.4	1.0	10	-8.548e-5	3.575e-4	6.910e-5
0.5	1.0	10	-1.4417e-4	2.769e-4	5.543e-5
0.6	1.0	50	-7.926e-4	8.303e-4	1.674e-4
0.7	1.0	50	-6.057e-4	4.340e-4	3.446e-7
0.8	1.0	50	-4.221e-4	3.440e-4	-1.331e-4
0.9	1.0	100	-5.087e-4	7.218e-4	-4.042e-4

REFERENCES

Ahrens, T. J., Harris, A. W., Deflection and Fragmentation of Near-Earth Asteroids, In *Hazards Due to Comets and Asteroids*, ed. T. Geherls, Univ. of Arizona Press, 1994, pp. 897-928.

Bowell, E., Muinonen, K., Earth-Crossing Asteroids and Comets: Groundbased Search Strategies, In *Hazards Due to Comets and Asteroids*, ed. T. Geherls, Univ. of Arizona Press, 1994, pp. 149-198.

Brown, C. D., *Spacecraft Mission Design*, American Institute of Aeronautics and Astronautics, Inc., Washington, DC, 1992.

Canavan, G. H., Solem, J. C., Rather, J. D. G., Near-Earth Object Interception Workshop, In *Hazards Due to Comets and Asteroids*, ed. T. Geherls, Univ. of Arizona Press, 1994, pp. 93-124.

Carusi, A., Gehrels, T., Helin, E. F., Marsden, B. G., Russell, K. S., Shoemaker, C. S., Shoemaker, E. M., Steel, D. I., Near-Earth Objects: Present Search Programs, In *Hazards Due to Comets and Asteroids*, ed. T. Geherls, Univ. of Arizona Press, 1994, pp. 127-148.

Cheng, A. F., Veverka, J., Pilcher, C., Farquhar, R. W., Missions to Near-Earth Objects, In *Hazards Due to Comets and Asteroids*, ed. T. Geherls, Univ. of Arizona Press, 1994, pp. 651-670.

Elder, J. T., *Optimal Impulse Conditions for Deflecting Earth Crossing Asteroids*, Master's Thesis, Naval Postgraduate School, 1997.

Greenwood, D. T., *Principles of Dynamics*, Prentice Hall, Englewood Cliffs, New Jersey, 1988.

Hills, J. G., Goda, M. P., The Fragmentation of Small Asteroids in the Atmosphere, *The Astronomical Journal*, vol. 105, no. 3, pp. 1114-1144, (1993).

Janes Strategis Weapons Systems, Issue 23, January, 1997, Jane's Information Group, Couldson, Surrey, U.K.

Knudson, W. E., *Orbital Perturbation Analysis of Earth-Crossing Asteroids*, Master's Thesis, Naval Postgraduate School, 1995.

Medwin, Thomas, *Journal of the Conversations of Lord Byron: Noted During a Residence with His Lordship at Pisa, In the Years 1821 and 1822*, printed for Henry Colburn, New Burlington Street, London, 1824.

Meissinger, H. F., *Technology Assessment for Defense Against Asteroids or Comets*, briefing slides for the Planetary Defense Workshop, Livermore, CA, May 22-26, 1995.

Melosh, H. J., Nemchinov, I. V., Zetzer, Yu. I., Non-Nuclear Strategies for Deflection Comets and Asteroids, In *Hazards Due to Comets and Asteroids*, ed. T. Geherls, Univ. of Arizona Press, 1994, pp. 1111-1132.

Morrison, D., Chapman, C. R., Slovic, P., The Impact Hazard, In *Hazards Due to Comets and Asteroids*, ed. T. Geherls, Univ. of Arizona Press, 1994, pp. 59-92.

NASA Ames website, *Asteroid and Comet Impact Hazard*, http://george.arc.nasa.gov/sst/

Park, S. Y., Elder, J. T., Ross, I. M., *Minimum Delta-V for Deflection Earth-Crossing Asteroids*, AAS/AIAA Astrodynamics Specialist Conference, 4-7 August, 1997, Sun Valley Idaho.

Rabinowitz, D. L., Bowell, E., Shoemaker, E. M., Muinonen, K., The Population of Earth-Crossing Asteroids, In *Hazards Due to Comets and Asteroids*, ed. T. Geherls, Univ. of Arizona Press, 1994, pp. 285-312.

Rustan, P. L., Space Launch Vehicles, In *Hazards Due to Comets and Asteroids*, ed. T. Geherls, Univ. of Arizona Press, 1994, pp. 1065-1072.

Simonenko, V. A., Nogin, V. N., Petrov, D. V., Shubin, O. N., Solem, J. C., Defending the Earth Against Impacts from Large Comets and Asteroids, In *Hazards Due to Comets and Asteroids*, ed. T. Geherls, Univ. of Arizona Press, 1994, pp. 929-954.

Solem, J. C., Snell, C. M., Terminal Intercept for Less Than One Orbital Period Warning, In *Hazards Due to Comets and Asteroids*, ed. T. Geherls, Univ. of Arizona Press, 1994, pp. 1013-1034.

Shafer, B. P., Garcia, M. D., Scammon, R. J., Snell, C. M., Stellingwerf, R. F., Remo, J. L., Managan, R. A., Rosenkilde, C. E., The Coupling of Energy to Asteroids and Comets, In *Hazards Due to Comets and Asteroids*, ed. T. Geherls, Univ. of Arizona Press, 1994, pp. 955-1012.

Teller, E., Ishikawa, M., Wood, L., Hyde, R., *Cosmic Bombardment V: Threat Object-Dispersing Approaches to Active Planetary Defense*, for the Planetary Defense Workshop, Livermore, CA, May 22-26, 1995.

Wiesel, W. E., *Spaceflight Dynamics*, McGraw-Hill, New York, 1997.

Willoughby, A. J., McGuire, M. L., Borowski, S. K., Howe, S. D., The role of Nuclear Thermal Propulsion in Mitigating Earth-Threatening Asteroids, In *Hazards Due to Comets and Asteroids*, ed. T. Geherls, Univ. of Arizona Press, 1994, pp. 1073-1088.

Wood, L. L., Hyde, R., Ishikawa, M. Y., Ledebuhr, A., *Cosmic Bombardment IV: Averting Catastrophy in the Here-and-Now*, A Presentation To: Problems of Earth Protection Against The Impact With Near-Earth Objects (SPE-94), September 26-30, 1994, LLNL Doc. No. PHYS. BRIEF 94-029.

Yeomans, D. K., Chodas, P. W., Predicting Close Approaches of Asteroids and Comets to Earth, In *Hazards Due to Comets and Asteroids*, ed. T. Geherls, Univ. of Arizona Press, 1994, pp. 241-258.

BIBLIOGRAPHY

Larson, W. J., Wertz, J. R., Editors, *Space Mission Analysis and Design*, Kluwer Academic Publishers, Boston, 1992.

Vallado, D. A., *Fundamentals of Astrodynamics and Applications*, McGraw-Hill, New York, 1996.

INITIAL DISTRIBUTION LIST

Number of Copies

1. Defense Technical Information Center...2
   8725 John J. Kingman Rd., STE 0944
   Ft. Belvoir, Virginia 22060-6218

2. Dudley Knox Library..2
   Naval Postgraduate School
   411 Dyer Rd.
   Monterey, California 93943-5101

3. Department Chairman, Code AA...1
   Department of Aeronautics and Astronautics
   Naval Postgraduate School
   Monterey, California 93943-5000

4. Department of Aeronautics and Astronautics...5
   Attn: Professor I. M. Ross, Code AA/Ro
   Naval Postgraduate School
   Monterey, California 93943-5000

5. Department of Aeronautics and Astronautics...1
   Attn: Dr. S. Y. Park
   Naval Postgraduate School
   Monterey, California 93943-5000

6. HQ SWC/AES...1
   Joseph Liu
   730 Irwin Avenue, Suite 83
   Falcon AFB, CO 80912-7383

7. Lieutenant Scott D. V. Porter, USN.......................................3
   5552 Caminito Roberto
   San Diego, California 92111